HAL
open science

Development of pyrene-based fluorescent ether lipid as inhibitor of SK3 ion channels

Alicia Bauduin, Marion Papin, Aurélie Chantôme, Hélène Couthon, Laure Burel-Deschamps, Jose Requejo-Isidro, Christophe Vandier, Paul-Alain Jaffres

To cite this version:

Alicia Bauduin, Marion Papin, Aurélie Chantôme, Hélène Couthon, Laure Burel-Deschamps, et al.. Development of pyrene-based fluorescent ether lipid as inhibitor of SK3 ion channels. European Journal of Medicinal Chemistry, 2021, 209, pp.112894. 10.1016/j.ejmech.2020.112894 . hal-02997273

HAL Id: hal-02997273

https://hal.univ-brest.fr/hal-02997273

Submitted on 17 Oct 2022

HAL is a multi-disciplinary open access archive for the deposit and dissemination of scientific research documents, whether they are published or not. The documents may come from teaching and research institutions in France or abroad, or from public or private research centers.

L'archive ouverte pluridisciplinaire **HAL**, est destinée au dépôt et à la diffusion de documents scientifiques de niveau recherche, publiés ou non, émanant des établissements d'enseignement et de recherche français ou étrangers, des laboratoires publics ou privés.

Distributed under a Creative Commons Attribution - NonCommercial 4.0 International License

Version of Record: https://www.sciencedirect.com/science/article/pii/S0223523420308667
Manuscript_5ff2c52b1cdd5bfaae4a9149d3a32286

Development of pyrene-based Fluorescent ether lipid as inhibitor of SK3 ion channels.

Alicia Bauduin,[a] Marion Papin,[b] Aurélie Chantôme,[b] Hélène Couthon,[a] Laure Deschamps,[a] Jose Requejo-Isidro,[c] Christophe Vandier,[b] Paul-Alain Jaffrès,[a*]

a) Univ Brest, CEMCA UMR CNRS 6521, 6 Avenue Victor Le Gorgeu, F-29238 Brest, France. E-mail: pjaffres@univ-brest.fr.

b) Univ Tours, Inserm U1069 Nutrition, Croissance et Cancer (N2C), Faculty of Medicine, 10 Boulevard Tonnellé, 37032, Tours Cedex, France.

c) Centro Nacional de Biotecnología (CNB), CSIC, Madrid, Spain; Unidad de Nanobiotecnología, CNB-CSIC-IMDEA Nanociencia Associated Unit, Madrid, Spain.

Abstract

We report the synthesis of three bioactive pyrene-based fluorescent analogues of Ohmline which is the most efficient and selective inhibitor of SK3 ion channel. The interaction of these Ohmline-pyrene (**OP1-3**) with liposomes of different composition reveals that only **OP2** and **OP3** are readily integrated into liposomes. Fluorescence measurements indicate that, depending on their concentration, **OP2** and **OP3** exist either as monomer or as a mixture of monomer and excimers within the liposome bilayer. Among the three Ohmline Pyrene compounds (**OP1-3**) only **OP2** is able to reduce SK3 currents and is the first efficient fluorescent modulator of SK3 channel as revealed by patch clamp measurements (- 71.3 ± 13.3 % at 10 µM) and by its inhibition of SK3-dependent cancer cell migration at (-32.5 % ± 4.8 % at 1 µM). We also report the first fluorescence study on living breast cancer cells (MDA-MB-231) showing that **OP2** is rapidly integrated in bio-membranes followed by cell internalization.

Keywords: glyco-glycerolipid; ether lipid; liposome; fluorescence; amphiphiles; SK3; ion channel

© 2020 published by Elsevier. This manuscript is made available under the CC BY NC user license
https://creativecommons.org/licenses/by-nc/4.0/

1. Introduction

The involvement of ion channels in cancer development [1-3], cancer cell migration [4-5] or cancer chemotherapeutic resistance [6-7] emerged over the last 20 years leading to the identification of novel targets and possibly new cancer treatments. Moreover, the modification of the expression of some ion channels is correlated to the aggressiveness of cancers and are thus studied as potential cancer biomarkers [8-9]. To the best of our knowledge, none of the ion channel modulators (mostly small molecules) currently on the market (e.g. type II diabetes, hypertension, pain, anxiety) [10] are used for cancer therapy except for the treatment of the side effects of chemotherapy (treatment of nausea *via* an antagonist effect on 5HT3 receptors). In our laboratories, we have previously reported for the first time that amphiphilic compounds belonging to the class of glyco-glycero ether lipids were able to modulate SK3 channels. SK3 channels (KCa2.3 ; small conductance K+ channel activated by cytosolic calcium) [11] are overexpressed in some cancer cells (e.g. breast MDA-MB-435s cells) and are associated to cancer-cell migration [12-13]. Ohmline (Figure 1) is one of the most efficient compounds [14] that selectively inhibits SK3 (73% of reduction of SK3 current according to patch clamp measurements at 10 µM) and that reduces SK3-dependent cancer-cell migration (50% according to a chronic test at 0.3 µM for 24h). These results were confirmed *in vivo* with a human cancer cell xenograft model in NMRI/nude mice that developed bone metastasis after 3 to 9 weeks. The treatment of these mice with Ohmline abolished the formation of bone metastasis without any visible side effects [15]. Subsequently, other analogues of Ohmline featuring different polar head groups (phospho-saccharide [16], digalactoside [17], other disaccharides [18] or more recently tetrahydropyrine [19]) were synthesized and were also able to inhibit SK3 ion channels but with a lesser efficiency or a lower selectivity. Opposite to tetraethylammonium (TEA) [20] or apamin [21] that inhibit SK3 respectively by a cork effect at the pore channel and via an allosteric mechanism, Ohmline proceeds differently because it is not able to displace apamin from SKCa channels [11]. The mechanism of action of Ohmline starts by its integration in membrane as confirmed by ^{2}H NMR studies in membrane models using deuterated Ohmline [22]. After integration in membrane, Ohmline reduced the order parameters of rigid membrane (e.g. rich in cholesterol- 30%; determined by ^{2}H NMR of membranes that include perdeuterated lipids as probe) whereas it has almost no effect on fluid membrane [22]. According to molecular dynamic studies, the integration of Ohmline in cholesterol-containing membranes induced a modification of the equilibrium position of cholesterol embedded in the

membrane [22]. Altogether, our previous studies suggest that Ohmline is able to modify the bio-physical properties of cholesterol-rich membrane and consequently the function of SK3 ion channels embedded in nanodomains enriched with cholesterol also named lipid rafts. We have also shown that Ohmline was able to dissociate Orai1-SK3 channel complexes that are localized in cholesterol-rich domains of plasma membranes of some cancer cells [15] and to modulate the action anti-EGFR monoclonal antibodies [23]. Altogether, different hypotheses exist to explain the effect of Ohmline. 1-Ohmline, after its integration in plasma membrane, could interact directly with SK3 channels and modulate SK3 currents via allosteric mechanism of action. However, we reported that the chirality at the *sn*-2 position of the glycerol has no effect on the efficacy of Ohmline [11]. This observation reduces the pertinence of this hypothesis since direct protein-antagonist interactions are frequently very sensitive to the absolute configuration of the antagonist. 2- Ohmline by modifying the fluidity of rigid membranes could destabilize SK3 channels (functional SK3 channels are constituted by the assembly - homo or hetero-tetramers- of four SK3 protein and are sensitive to cholesterol) [23]. 3- We cannot exclude either that the integration of Ohmline in the membrane could trigger endocytosis processes by acting on membrane curvature [24] or by other unidentified mechanism that could reduce the expression of SK3 channels at the plasma membrane. To investigate further the distribution of Ohmline at a cellular scale that could contribute to better understand its mechanism of action, the preparation of a fluorescent analogue of Ohmline was required. In this article, we report the synthesis and the fluorescence properties of three analogues of Ohmline featuring a pyrene moiety attached at the extremity of a short lipid chain (**OP1-3**, figure 1). Then, we report their action on SK3 ion channels and finally the kinetic of distribution of **OP2** at a cellular scale.

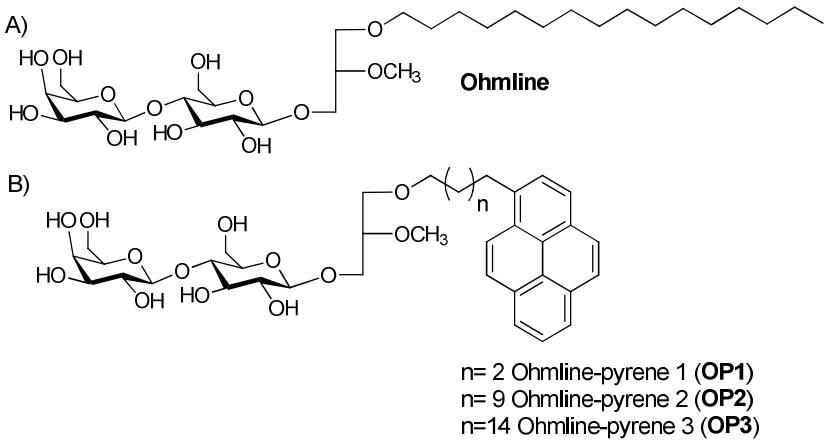

Fig. 1: Molecular structure of Ohmline and the fluorescent analogues **OP1-3**

2. Results and discussion

2.1 Synthesis

The introduction of a fluorescent probe on a bioactive compound presents the risk of reducing or abolishing its activity. For this reason, the structure of the fluorescent probe and its location on the molecular structure is of primary importance. In previous studies, we have shown the importance of the structure of the polar head group of the amphiphilic derivatives on their ability to modulate SK3 channels. This polar head group can be either a mono/di-saccharide unit or a phosphocholine moiety but in the latter case (e.g. Edelfosine) [25] higher toxicity was revealed. For the saccharide moiety, we have shown with Ohmline that the stereochemistry of the glycosylated link between the lactose and the glycerol unit was essential (only the stereoisomer β is active [18]). These results suggest that structural modifications on the polar head group could impair its capacity to modulate SK3 channels. Regarding the *sn*-2 position of the glycerol unit, we have first reported that the configuration of the carbon atom bearing the methoxy group had no effect on the capacity of Ohmline to modulate SK3 [11]. The presence of an unsubstituted alcohol in *sn*-2 position of a compound possessing a phosphocholine polar head group in *sn*-3 position produced a compound exempt of any activity on SK3. Accordingly, we would like to keep unchanged the methoxy group present on the *sn*-2 position of glycerol. Regarding the structure of the hydrophobic moiety, a straight and saturated lipid tail with a minimum of 16 carbon atoms is suitable. We suppose that this lipid chain acts as an anchor of the molecule in membranes. Altogether, we hypothesized that the best location for the fluorescent probe could be on the lipid chain. Previously, the functionalization of the lipid chain of Edelfosine was achieved by a polyene [26], polyene-yne or BODIPY [27] fluorescent moiety but the stability of some of these chromophores limited their use. Accordingly, we have selected pyrene, which was largely employed to label lipids to study membranes and cell biology [28]. Pyrene is a hydrophobic fluorescent probe that readily forms excimers featuring an intense fluorescence (emission at 470 nm) [29]. To determine the best position of the pyrene moiety in the structure of the lipid chain, we considered that its introduction as a ramification of a straight lipid chain could induced important modification of the supramolecular interactions as previously observed with branched amphiphiles [30]. On the other hand, the proximity of the pyrene group to the glycerol would require a di-substituted pyrene (one to connect pyrene to glyceryl and a second to place a lipid chain) which is a more difficult option from a synthesis point of view

[31]. Hence, we have selected to place the pyrene moiety at the extremity of the lipid chain. First, we used pyrene methanol as commercial precursor because it was previously used to prepare pyrene conjugates [32-33]. Accordingly (Figure S1-1), solketal was alkylated with 11-Bromoundecanol to produce the lipid alcohol **1** which was converted in bromo derivative **2** by using Appel's reaction. Pyrene methanol was then used as nucleophile to produce the pyrene-lipid intermediate **3**. However, the deprotection of the acetal function of **3** with either HCl/methanol or acetic acid (80%) produced a mixture of compound likely due to the reactive ether position close to the pyrene moiety. The cleavage of part of this ether position is likely due to its benzylic position that after protonation promotes its cleavage. In consequence, we modified the synthesis scheme to avoid the incorporation of heteroatom in the hydrophobic moiety. As shown in Figure 2, we first prepared the pyrene derivatives **4a-c** that feature a straight alkyl chain separating the pyrene moiety to the bromine atom.

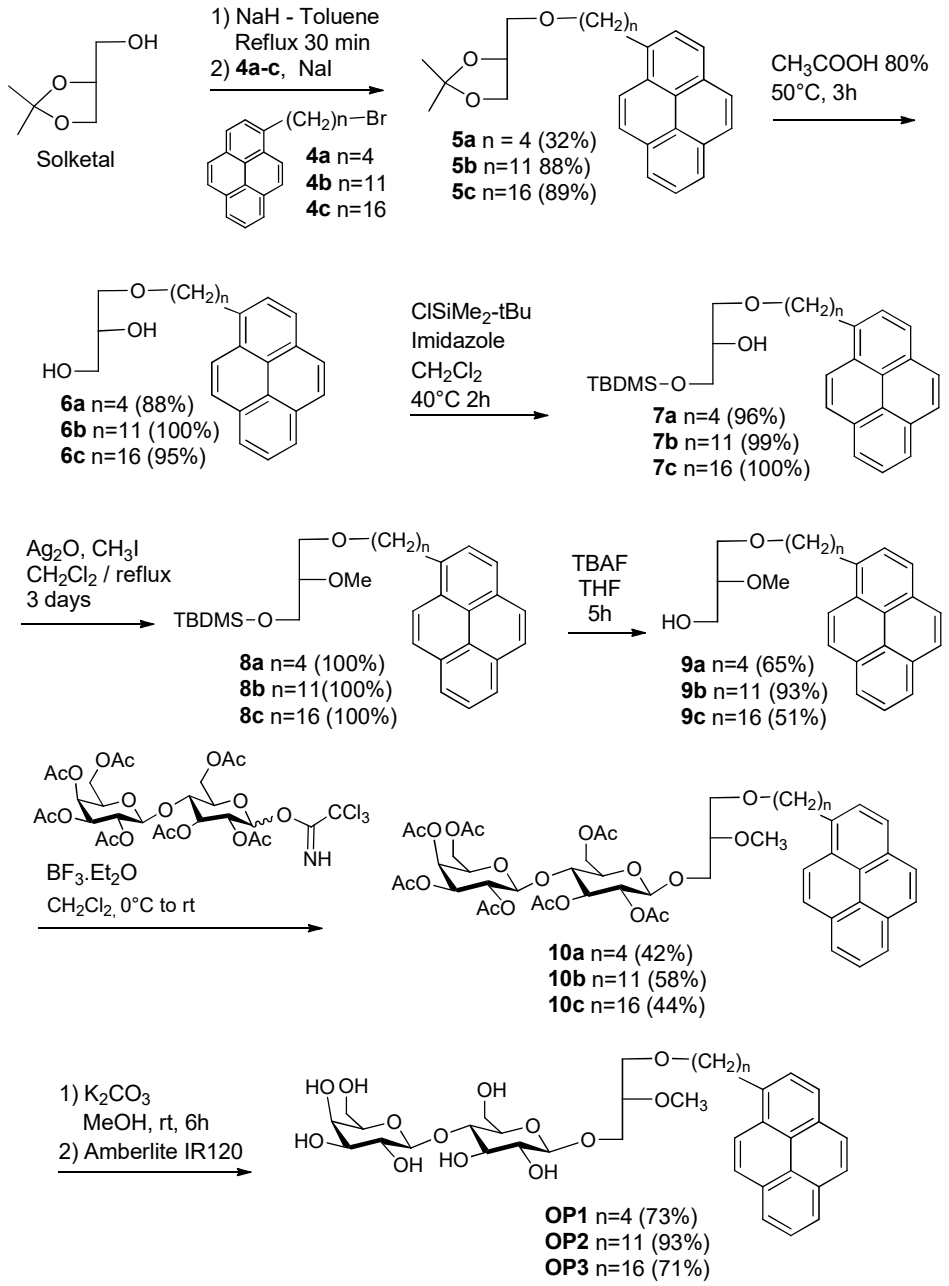

Fig. 2: Synthesis of the fluorescent Ohmline-Pyrene **OP1-3**

The constitution of this alkyl chain, that can influence the modulation effect on SK3, contains either 4, 11 or 16 methylene units. **4a** was prepared from pyrene-butanol as previously reported [34] and **4b-c** were prepared by adapting reported procedures [35] using pyrene as substrate (Figure S2-1). Then, solketal (racemic) was deprotonated by NaH in toluene and reacted with **4a-c** in presence of NaI to produce **5a-c**. The deprotection of the acetal **5b** in presence of 12M HCl (procedure used for the preparation of Ohmline) failed in the present case. Accordingly, we used acetic acid to produce **6a-c** in excellent yield. Then,

the protection of the primary alcohol was attempted with trityl protecting group but we faced low and unreproducible yields. Accordingly, we used *t*-butyldimethylchlorosilane and imidazole in dichloromethane [36] to protect the more reactive alcohol to produce **7a-c** in nearly quantitative yield without any trace of migration of silyl group at the *sn*-2 position as it was previously reported in different reaction conditions [37]. Of note, a second protocol was developed for the preparation of **7a** by reaction of pyrenebutanol (Figure S3-1) with silylated glycidol but the yield was low (21%). Then, we applied a methylation with silver oxide and iodomethane [38] that produced **8a-c** in nearly quantitative yields. The methylation protocol used for the synthesis of Ohmline (NaH, THF and then methyliodide) was not efficient. The deprotection of the primary alcohol in presence of *n*-tetrabutylammonium fluoride (TBAF) produced **9a-c** in 51 to 93% yield. The glycosylation of **9a-c** was achieved with the same condition than for Ohmline (trichloroacetimidate derivative of per-acetylated lactose in presence of BF_3) produced **10a-c** in 42 to 58 % yield. Finally, the deprotection of the hydroxyl groups present on the lactose unit was achieved with a catalytic amount of potassium carbonate in methanol. After neutralization with Amberlite IR120H acid resin **Ohmline-Pyrene 1-3** (**OP1-3**) were isolated in 71 to 93% yield. As previously reported for the glycosylation reactions involving per-acetylated lactose, only the β-stereoisomer was formed likely due to the assistance of the adjacent acetyl group [39]. This stereochemistry was determined on **OP1-3** by ^{13}C-^{1}H NMR or "gated decoupling" experiment. The value of 160 Hz for the $^{1}JC_1$-H_1 coupling constant indicates an axial proton i.e the β-stereoisomer. Moreover, the chemical shifts (^{13}C NMR) of the anomeric carbons are between 103.8 and 102.9 ppm for **OP-1**, **OP-2** and **OP-3**, which are characteristics of β-linkage whereas chemical shift between 99 and 101 ppm is an indication of an α-linkage [40]. All the NMR spectra of compounds **5b**-**10b** and final compounds are presented in figures S4.

2.2 Fluorescence and interaction with liposomes

Then, we have recorded the fluorescence (Figure 3; gain of the detector either 600 or 800) of compounds **OP1-3** (excitation at 331 nm) in water at different concentration (0.1, 0.2 and 0.4 μM). It is observed that the fluorescence of the monomers is characterized by emission ranging from 360-440 nm whereas the excimer emission is characterized by a broad band from 425 to 600 nm [41-43]. It is clearly observed that **OP1**, which features the shortest alkyl spacer (4 methylene units), only exists as monomer at these concentrations. The fluorescence of **OP2** features only the signature of the monomer at 0.1 μM but at higher concentration,

both monomer and excimer are detected. The presence of the excimer is attributed to its higher hydrophobicity (the spacer contains 11 methylene units) that promotes its self-assembly in water. For **OP3**, which possesses the longest spacer (16 methylene units), the excimer is predominant even at the lowest concentration suggesting that at 0.1 µM this compound forms aggregates [35].

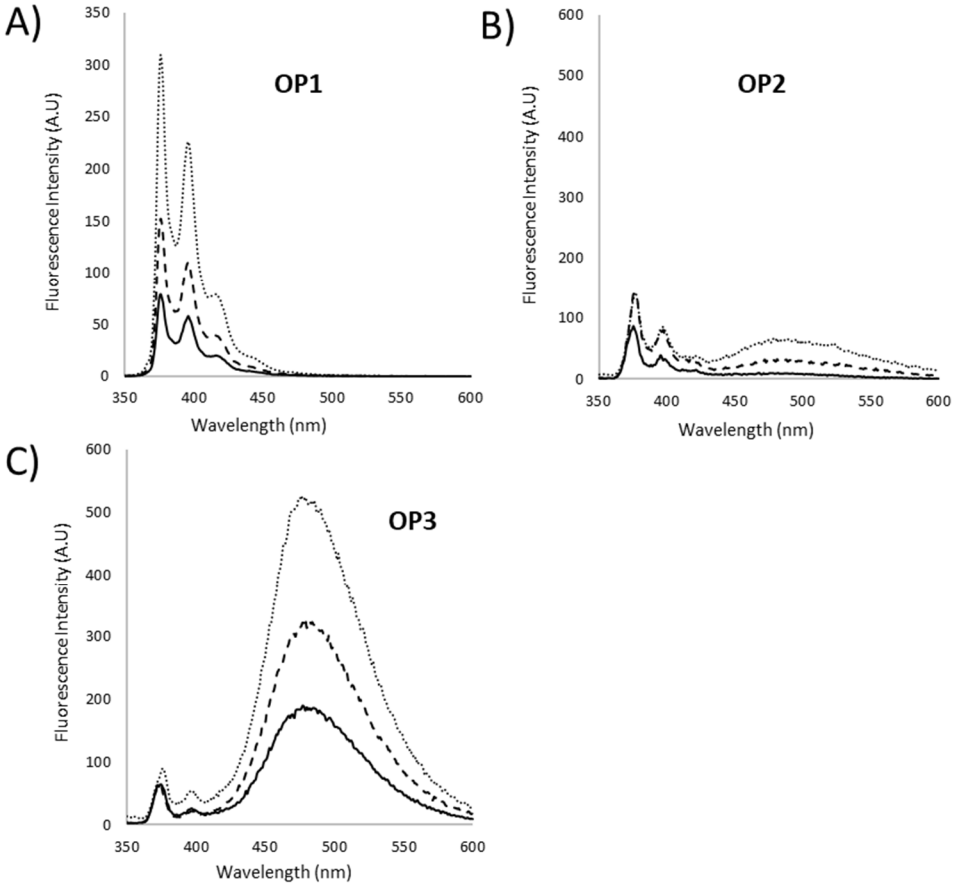

Fig. 3. Fluorescence spectra of compounds **OP1-3** after excitation at 331 nm and at different concentrations in water: 0.1 µM (solid line), 0.2 µM (dashed line) 0.4 µM (dotted line) ~~mol.L-1~~ A) **OP1** (gain of the detector 600); B) **OP2** (gain of the detector 800); C) **OP3** (gain of the detector 800).

Then, we investigated the fluorescent properties of compounds **OP1-3** placed in a lipid environment. For that study, we used liposomes of different compositions as a model of plasma membrane and we used two strategies to incorporate **OP1-3** in the liposomes. A first protocol (pre-insertion) involved to mix one of the OP compound with the other lipids (e.g. DOPC, DOPC/Cholesterol -70/30 mol % or Egg-PC) before the formation of the liposomes.

The second protocol involved to add one of the **OP** compounds on the liposomes already formed (post-insertion). According to the first protocol, one of the compound **OP1-3** was mixed with either DOPC, DOPC/Cholesterol (70/30 mol %), Egg-PC or Egg-PC/Cholesterol (70/30 mol %) to form a lipid film that produced liposomal solutions after hydration and sonication. In these formulations, the final concentration of **OP** compounds was 0.2 µM and the concentration of lipid either 8 µM, 24 µM and 40 µM. Accordingly, the lipid/**OP** molar ratios are 40, 120 and 200. For the second protocol (post-insertion) one of the **OP** compound, dissolved in a few µL of methanol, is added on liposomal solution (3 mL) at the same composition and concentration than those used for the pre-insertion protocol. The pre-insertion protocol aims to mimic the homogeneous distribution of **OP** compounds in the liposomes whereas the post-insertion protocol allows taking into account the migration process of **OP1-3** compounds from the solution to the liposomes.

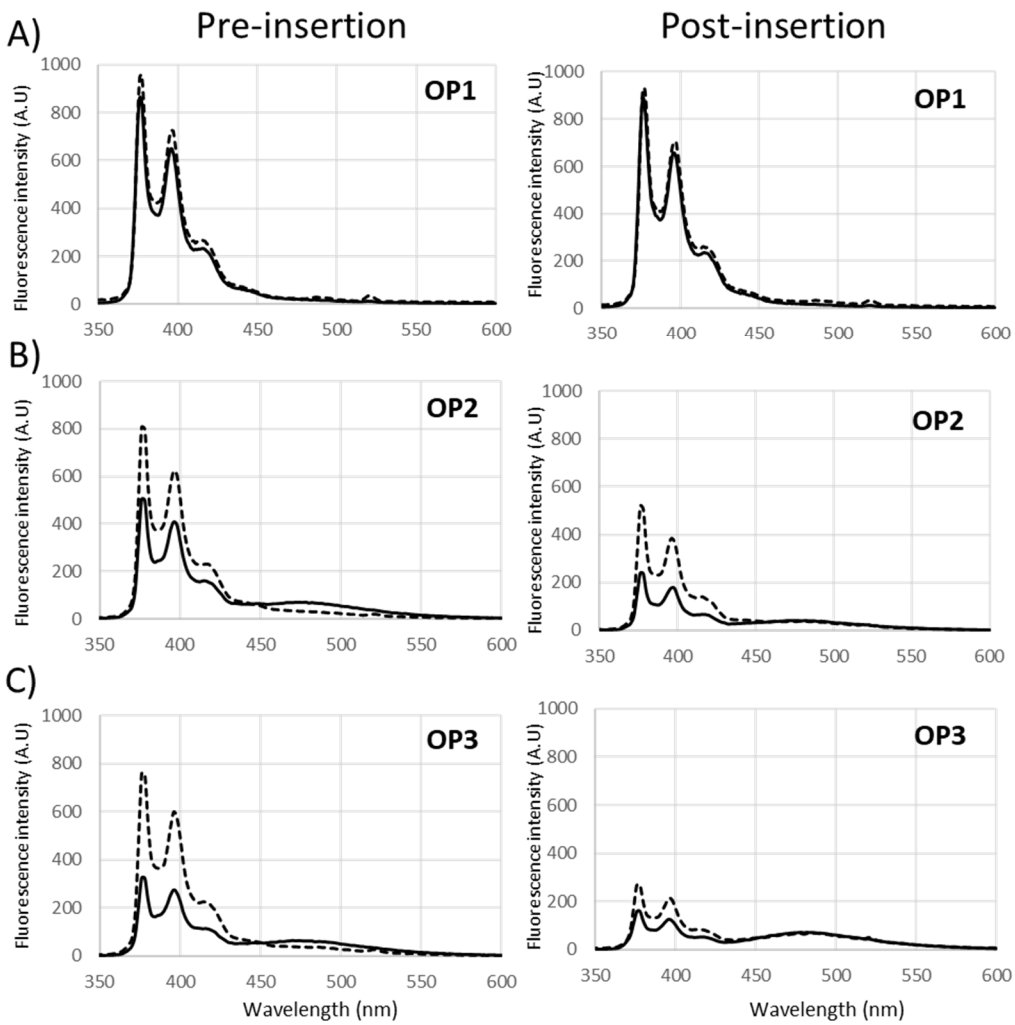

Fig. 4: fluorescence spectra (excitation at 331 nm) of **OP1-3** (0.2 µM) integrated in egg-PC-based liposomes at two concentrations 8 µM and 40 µM producing final ratios egg-PC/**OP** = 40 (solid line) and 200 (dashed line); gain of the detector: 750. Two protocols were used: pre-insertion (left column) and post-insertion (right column) A) **OP1** , B) **OP2**, C) **OP3**.

For the pre-insertion procedure (figure 4, left column, gain of the detector 750) with compounds **OP2** and **OP3** the fluorescence intensity of the monomer increases when the lipid/**OP** ratios increase from 40 to 200 whereas the fluorescence of the excimer decreases. This shows that both compounds, whose fluorescence in water are very low (figure 3), are inserted in the liposomes and that they only exist as monomer for highest dilution (high lipid/**OP** ratio of 200). When the lipid/**OP** ratio decreases the fluorescence of both monomers and excimers are observed in the liposomes suggesting some proximity of the pyrene-based compounds.

For **OP1** the result is completely different. Only the fluorescence of the monomer is observed irrespective of the two lipid/**OP1** ratios and the intensity of fluorescence is almost identical in both cases. These results suggest that either **OP1** is integrated in the liposomes but it is fully disperse thus rendering the proximity of the pyrene probe unlikely and the excimer absent or, more likely, **OP1** is, at this concentration (0.2 µM), fully soluble in water. Therefore, **OP1** escapes from the liposomes to be present in water.

For the post-inserted procedure (Figure 4, right column), the fluorescence intensity of the monomer is, lower than for the pre-inserted procedure (for the ratio egg-PC/**OP** 200) for **OP2** and **OP3**. This expected result is explained by the fact that according to the post-insertion protocol, a full distribution within the two leaflets requires flip-flop processes that likely require a longer time. It represents almost 65% of the signal obtained for the pre-insertion method for **OP2** and 35% for **OP3**. Since the fluorescent intensity of the monomer of **OP2** and **OP3** in water is very low (Figure 3B-C), this result suggests that **OP2-3** compounds are integrated, at least partly, in the liposome bilayer. The evolution of the ratio of **OP2** or **OP3** existing as monomer or excimer in liposomes can be evaluated by measuring the ratio of intensity I_{376}/I_{484}. For lipid/**OP** ratio equal to 200 (highest dilution), the ratio of intensity I_{376}/I_{484} is equal to 21 for the pre-insertion procedure for both compounds and to 8.5 for **OP2** and 4 for **OP3** for the post-insertion protocol. This result indicates that: 1- the post-insertion protocol produces a more heterogeneous distribution of **OP2** and **OP3** within the lipid bilayer since the signal of the excimer is more intense when compared to the pre-insertion protocol

that promotes homogeneous distribution of the **OP** compounds within the liposome bilayer. ~~2- The relative intensity of fluorescence (monomer + excimer) after post-insertion of **OP2** versus **OP3** suggests that **OP2** integrates the lipid bilayer more efficiently than **OP3**~~. 2- The more hydrophobic nature of **OP3** suggests that in water **OP3** is more aggregated and consequently could integrate the liposomes with a higher aggregation state or feature lower mobility within the bilayer thus producing a relative lower value for the ratio I_{376}/I_{484} when compared to **OP2**. To evaluate this second hypothesis, we recorded the size of the nano-objects by dynamic light scattering (DLS) for the three samples **OP1-3** in water at 4 different concentrations (40 µM, 10µM and 1µM ; Table S1). We found that only **OP2** and **OP3**, at the concentration of 40 µM and 10 µM, produced nano-objects with a repeatable size (Table S1). We observed that at these two concentrations **OP2** produced nano-objects featuring a size close to 50 nm whereas **OP3** produced larger nano-objects (close to 160 nm). These results are therefore consistent with the interpretation of the fluorescence data.

For **OP1**, the post-insertion procedure produced similar fluorescence spectra than with the pre-insertion procedure. In that case also, the lipid/**OP1** ratio has no effect on the fluorescence spectra. These results suggest that **OP1** is likely not integrated in the liposomes and the absence of excimer suggests that at this concentration (0.2 µM) **OP1** is not aggregated in water.

Similar experiments were carried out with different liposomal formulations. For **OP1**, which seems to be mainly localized in water (figure 4A), the same conclusions were obtained with Egg-PC/cholesterol (70/30 mol ratio) liposomal solution. Only the signature of the monomer was detected and the intensity ratio were identical when using the pre-insertion or post-insertion protocols (Figure S5-1). For **OP2** and **OP3**, we tested EggPC/Cholesterol (70/30), DOPC and DOPC/Cholesterol 70/30 (Figure S6-1 and Figure S7-1). Similar trends than those reported in Figure 4B and 4C were observed suggesting that the composition of the liposomal formulation has a weak effect on the incorporation of these amphiphiles irrespective the protocol used (pre or post insertion). Altogether, the fluorescence analysis of **OP1-3** in different liposomal compositions indicates that **OP1** is likely not integrated in the liposomes. On the contrary, **OP2** and **OP3** are able to integrate in the liposomes irrespective to both the protocol used (pre or post-insertion) and the composition of the liposomes. However, the integration rates of **OP2** and **OP3** are slightly higher with the pre-insertion protocol.

2.3 Effect of **OP1-3** on SK3

Then, compounds **OP1-3** were evaluated for their capacity to modulate the activity of SK3 channels using the whole cell configuration of the patch clamp technique. Using this technique HEK293 cells (cells that overexpressed SK3 channel) were placed under acute condition (high concentration of **OP2** 10 µM, and 1 min. until the steady state reached). Figure 5A shows typical currents recorded at membrane potentials varying from -100 to +100 mV for 500 ms in control condition, after application of **OP2** compounds, and after application of apamin at the end of experiment. Apamin was used to inhibit SK3 residual current which was not sensitive to **OP2**. As illustrated **OP2** reduced most of the amplitude of SK3 currents but not totally as shown by the additional inhibition of residual SK3 currents by apamin. Figure 5B shows that **OP2** (10 µM) reduced SK3 currents by -71.3% (± 13.3%; N=6) and with a maximal effect of **OP2** compound attempted in one minute. In contrast to **OP2**, **OP1** and **OP3** had no effect on SK3 currents (Figure S8). These results emphasize the importance of the length of the linker between the pyrene moiety and the glycerol backbone since only **OP2**, featuring 11 methylene units in the spacer, is efficient. The importance of the aliphatic chain length between the pyrene and the glycerol unit on the modulation of SK3 could be explained as follow : 1- in the case of a short aliphatic chain (**OP1**), the hydrophobic domain is too short to localized **OP1** in the bilayer as demonstrated by fluorescence. Accordingly, **OP1** do not modify the lipid-bilayer biophysics and therefore has no effect on SK3 function. 2- in the case of a long aliphatic chain (**OP3**), it is likely that the hydrophobic domain length (aliphatic chain and pyrene) is longer than the average of the lipid chain of phospholipid or sphingosine derivatives present in bio-membranes. In consequence, the hydrophobic chain of **OP3** must adopt either a U-shape conformation to keep its hydrophobic chain within one leaflet or has a hydrophobic domain that cross over the inter-leaflet area; in both cases the effect on bio-membrane biophysics will be different to **OP2**, which has a hydrophobic chain length almost similar to those of the phospholipid present in the membrane.

Then, we studied the effect of **OP2** on the migration of MDA-MB-435s that expressed (SK3+) or not SK3 channel (SK3-) (Figure 5C). **OP2** significantly reduces the migration of SK3+ cells at 1 µM (-32.5 % ± 4.8 %) but not at 0.3 µM in contrast to Ohmline, which is effective at 0.3 µM. Interestingly, **OP2** has no effect on the migration of SK3- cells demonstrating that this compounds inhibits SK3-dependent cancer cell migration as already observed with Ohmline [14]. In addition, the non-toxicity of the compounds **OP1-3** was confirmed at 1 µM by MTT assays (Figure S9). Altogether, these results show that although

having a slightly decrease efficiency in SK3 currents and SK3-dependent cancer cell migration compare to Ohmline, **OP2** is a molecule that opens major opportunities to investigate the cellular distribution of Ohmline and is the first fluorescent analogue of Ohmline reported so far.

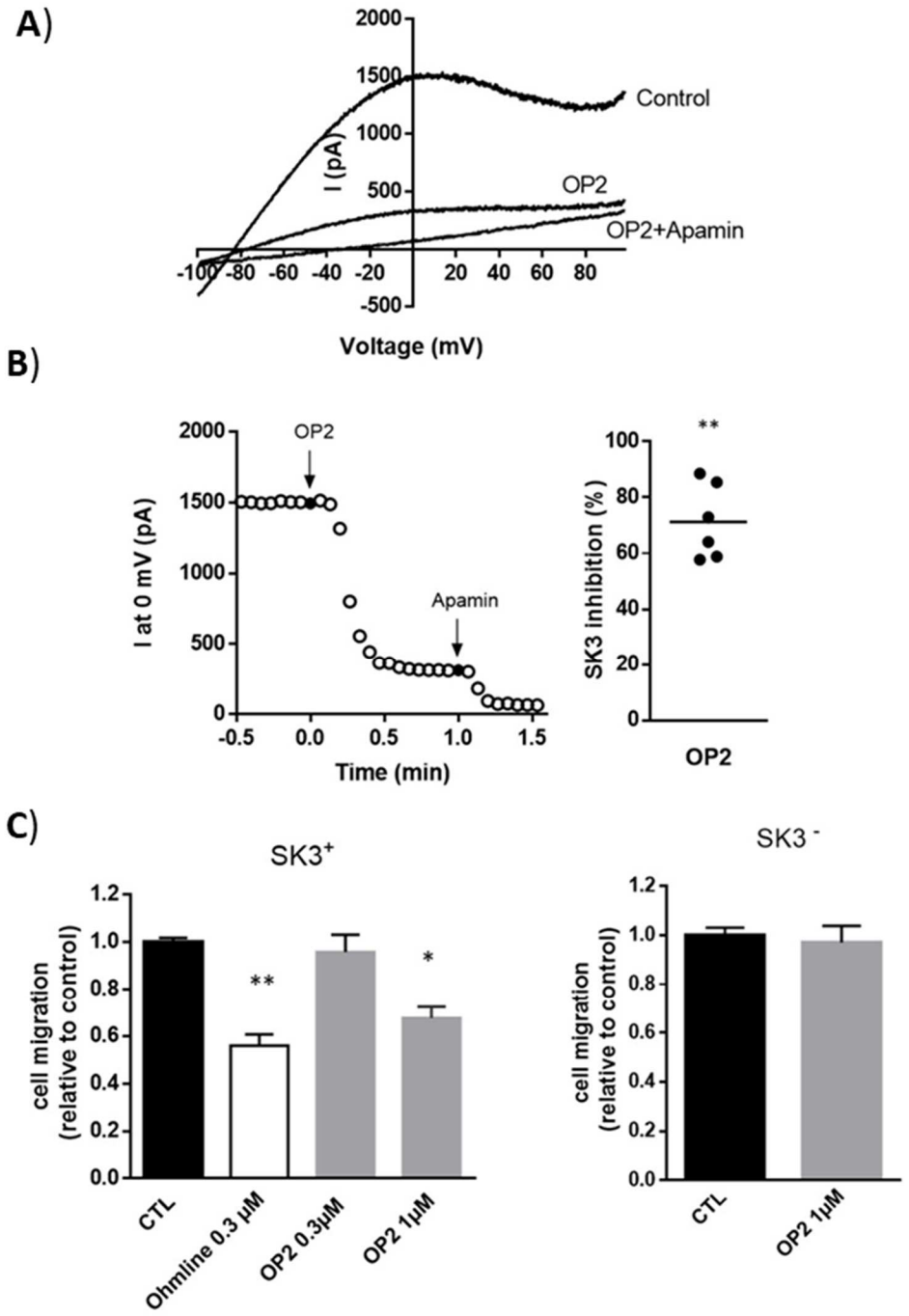

Fig. 5: Effects of **OP2** in SK3 currents and in SK3-dependent cancer cell migration. A) Representative whole-cell SK3 currents recorded at membrane potentials varying from +100 mV to -100 mV for 500 msec from a constant holding potential of 0 mV at pCa 6, before and

after application of 10 µM **OP2**, then with the addition of 0.1 µM apamin (SK3 peptide blocker) in HEK293T cells expressing recombinant rat SK3. B) Analyses of **OP2** effect on SK3 currents at 0 mV at 10 µM, a membrane potential where the current is only carried by SK3 channels. Left, graphs showing a representative time course of inhibitory effect of **OP2** on SK3 currents at 0 mV. Right, histograms showing the % of SK3 currents block by **OP2** when the steady-state inhibition was reached at I=0 mV. Lines indicate the median, each point represents the % of SK3 currents sensitive to **OP2** of each cell analyzed (N=6, ** $p < 0.01$, Wilcoxon signed rank test). C) Effect of **OP2** in SK3-dependent cell migration. Results are relative to control condition and are expressed as mean ± S.E.M. Left, histogram showing the effect of **OP2** and Ohmline in the cell migration of MDA-MB-435s expressing endogenous SK3 channels (SK3+). N=3, n=6 (CTL vs Ohmline 0.3 µM ** $p < 0.01$, CTL vs OP2 1 µM * $p < 0.05$, Dunn's multiple comparison test). Right, histogram showing no effect of **OP2** in the cell migration of MDA-MB-435s not expressing SK3 channel (SK3-). N=3, n=9 ($p > 0.05$, Mann-Whitney test).

2.4 *In vitro* fluorescence imaging.

To further understand **OP2** effects on cells, we imaged **OP2** excimers in breast cancer cells (MDA-MB-231) that had been treated with **OP2**. Two types of experiments were performed: (1) cells were imaged following addition of **OP2** to the medium and, (2) cells were left in an **OP2**-containing medium for 24h before imaging. In the former case, the serum supplemented medium used for cell culture was replaced with serum-free medium for **OP2** treatment (1 µM **OP2** total concentration); in the latter, **OP2** was added in serum supplemented medium and cells were incubated for a further 24h to test cellular viability (10 µM **OP2** total concentration). **OP2** incorporated into the cells within 45 min following treatment (figure 6a) and with an abundant distribution in the plasma membrane. At that time, background fluorescence could still be detected in the medium, indicating that **OP2** uptake was not yet complete. 24h after OP2 treatment cells (Figure 6b; **OP2** at 10 µM) the population of fluorescent cells had increased, indicating cells were healthy and viable, and no fluorescence background emission from the excimers could be observed from the medium. We note that the concurrent presence of **OP2** excimers and monomers in solution was already observed at a concentration 25 times lower (0.4 µM, Fig 3b, dotted line) and that the proportion of excimers to monomers increases with compound concentration. This, together with the large excimers background observed at short times after addition of **OP2** at 10 µM, strongly suggests that most of the compound is in excimers form at this concentration.

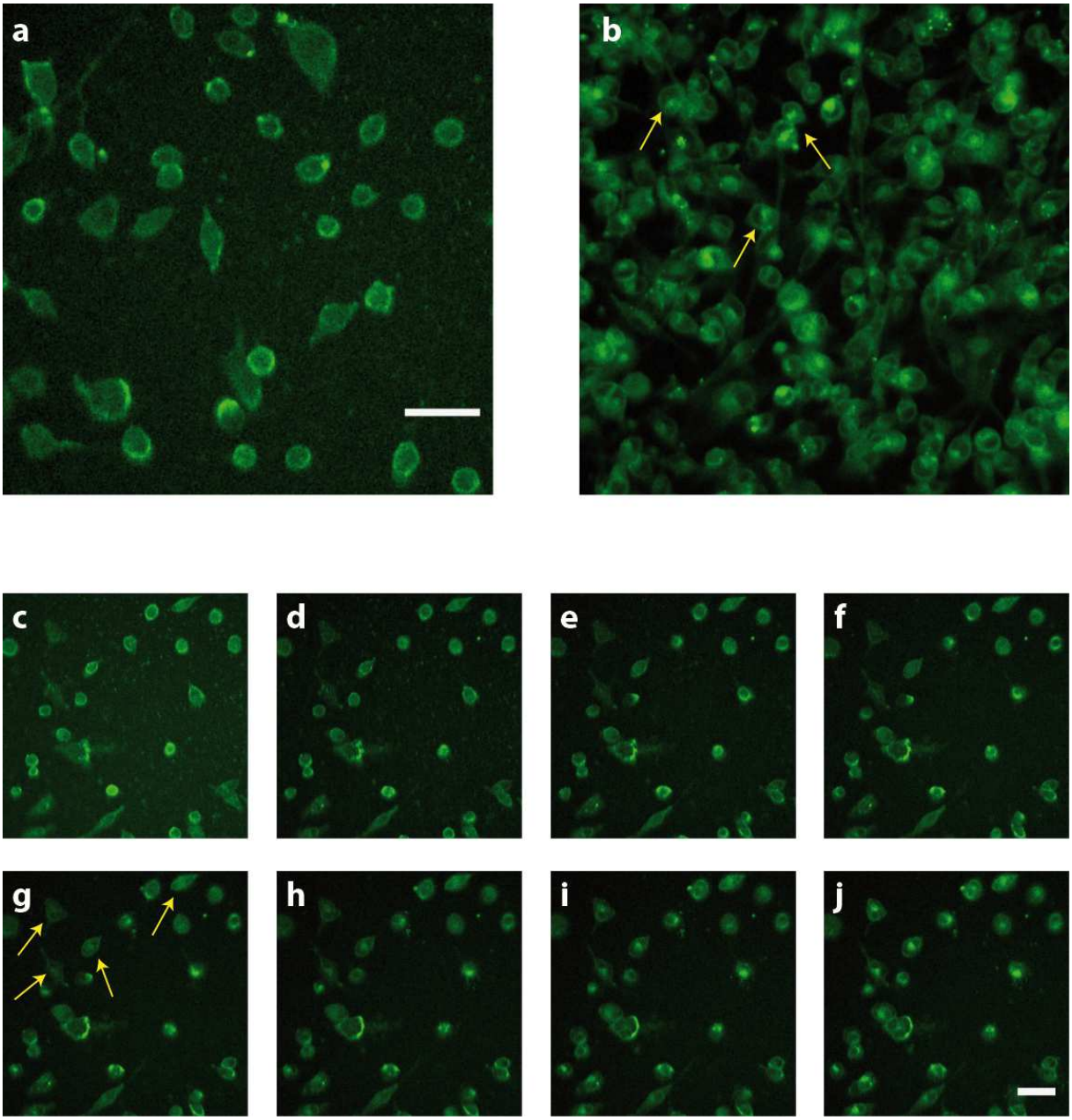

Fig. 6. **OP2** cellular uptake. **OP2** is internalized in MDA-MB-231 cells following its addition to the culture medium. (a) 45 min after addition of **OP2** at 1 µM (total concentration): Upon internalization, **OP2** distributes in the plasma membrane and in the cytoplasm, but it is not internalized in the cell nucleus. (b) Cells imaged 24h after treatment with **OP2** (10 µM), confirming cellular viability. (c-j) Cells were imaged every 15 minutes starting at (c) t_0=60 min following addition of **OP2** (1 µM total concentration), and finishing at (j) t_f=165 min after treatment. **OP2** accumulates in patches around the nucleus that start developing 2h after treatment (g, yellow arrows). (a-k) scale bar is 50 µm. Fluorescence excitation at 340 nm and emission recorded from 468 to 552 nm.

To further understand the dynamics of **OP2** cellular uptake, we imaged the same region of the culture dish every 15 min, starting 1 hour after treatment (Figure 6c-k). Background excimers emission was negligible 1.5h after treatment (Figure 6e), suggesting complete incorporation into the cells. **OP2** accumulation at the periphery of the nucleus was visible 2h after treatment (Figure 6g, yellow arrows) while the nuclei were not fluorescent. This accumulation was still observed 24h after treatment (Figure 6b, yellow arrows). Altogether, this study shows that **OP2** is rapidly incorporated in the lipid bilayer, since we clearly observed cell internalization within 45 minutes after addition of **OP2** even at the lowest concentration (1 µM). This rapid integration of **OP2** in the plasma membrane is consistent with the patch clamp measurements. The second point is that **OP2**, after a first location at the plasma membranes that occur in the first 2 hours, is then internalized close to the nucleus. However, it is difficult to accurately identify the cellular region where **OP2** accumulates. In a previous study focused on fluorescent analogues of Edelfosine, Mollinedo et al. reported that these fluorescent analogues of Edelfosine localized in mitochondria and that the internalization was mediated by lipid rafts [27]. In the case of Ohmline and **OP2**, further studies will be needed to established their exact location within the cell, but the fact that SK3 has been recently identified in mitochondria [44], the development of drugs that could modulate intracellular target represents a great potential.

In order to test if the decrease of the activity of SK3 channel by **OP2** may be due to a decrease in the expression of SK3 protein at the plasma membrane, we used the cell-surface protein expression with proteinase K cleavage assay as we described previously [25]. In the absence of proteinase K, SK3 ran at a molecular mass of 75 kDa, consistent with the full-length SK3 protein (Figure S10). The presence of proteinase K lead to a cleavage of SK3 protein located at the plasma membrane resulting to an apparent molecular mass of 55 KDa. Ohmline and **OP2** treatments both revealed a 55 KDa cleaved SK3 band in the presence of proteinase K demonstrating that these compounds did not change the expression of SK3 protein at the plasma membrane.

3. Conclusion

Ohmline is a neutral amphiphilic compound belonging to ether-lipids, which was found, at a non-toxic concentration, to inhibit SK3 channel and consequently to reduce cancer cell mobility. Previous studies have shown that this compound was integrated in membranes and increased the fluidity of rigid membranes. To get further information relative to the distribution of this compound at a cellular scale, we report herein the synthesis of fluorescent analogues of Ohmline and also propose a general synthesis scheme for the design of amphiphiles labelled with a pyrene moiety. To this goal, we have incorporated a pyrene moiety at the ω-position of the lipid chain bonded via an ether linkage to glycerol. The number of methylene units separating glycerol from the pyrene moiety was either 4, 11 or 16 leading respectively, after a seven-steps sequence, to the compounds Ohmline-Pyrene 1-3 (**OP1-3**). Then, we report the interaction of these compounds with liposomes as a mimic of plasma membrane. Thanks to the singular fluorescent properties of pyrene derivatives that informed on its aggregation state (isolated species versus excimers) and based on two types of protocols for the incorporation of the fluorescent compounds in the liposomes (pre or post-insertion), we found that **OP1** (compound with the shortest lipid chain) is not integrated in the liposome. On the opposite, **OP2** and **OP3**, following the post-insertion protocol, integrate within liposomes with some aggregation. We also found that **OP2** integrates in the liposomes more efficiently thus emphasizing the effect of the length of the tether between the glycerol and the pyrene moiety on the supramolecular properties of this series of compounds. The three compounds **OP1-3** were tested as modulators of SK3. We found that only **OP2** (possessing 11 methylene units) is able to modulate SK3 (-71.3 % ± 13.3 at 10 µM) and to reduce SK3 dependent cancer cell migration (-32.5 % ± 4.8 % at 1 µM). **OP2** is therefore the first fluorescent analogue of Ohmline, which is able to modulate SK3 channel. In the last part of this study, we used fluorescent microscopy to track **OP2** over time. We found that, in agreement with patch clamp measurements, **OP2** is readily integrated in the plasma membranes and, after 2h, cell internalization occurred. The exact location of **OP2** into the cell will need further study but opens a new perspective for the modulation the SK3 channels localized in intercellular compartments.

4. Experimental protocols

4.1 Chemistry

4.1.1 General experimental protocols

Solvents were dried with a solvent purification system MBraun-SPS (toluene, CH_2Cl_2, THF) or freshly distilled on appropriate driers. All compounds were fully characterized by ^1H (500.133, 399.922 or 300.131 MHz) and ^{13}C NMR (125.803 or 75.474 MHz) NMR spectroscopy (Bruker AMX-3 300, Avance 400, Avance 500 and DRX 500 Spectrometers). Chemical shifts δ are given in ppm. Coupling constants J are given in hertz. The following abbreviations were used: s for singlet, d doublet, t triplet, q quadruplet, qt quintuplet, m multiplet, dd doublet of doublet, dt doublet of triplets. When needed, ^{13}C Heteronuclear HMQC and HMBC were used to unambiguously establish molecular structures. Mass spectrometry analyses were performed by Bruker Autoflex MALDI TOF-TOF (Brest University) Matrix used UTL HCCA. The size of the nano-objects were determined at 25°C in water by DLS with a NanoZS equipment (Malvern). The melting points were measured by a kofler bench. Molecular sieve (5Å) was used when indicated; Lactose trichloroacetimidate was prepared following reported procedure [45]. The pyrene derivatives **4a** was prepared following a reported procedure [35].

4.1.2. General procedure for the insertion of the 2,2-Dimethyl-1,3-dioxolane (Compounds **5a-c**):

NaH (5.5 eq.) was placed under nitrogen in a three-neck-round bottom flask fitted with a reflux condenser and an additional funnel. 10 mL of toluene were added. Solketal (5 eq.) was added and the mixture was refluxed for 1 h. At room temperature, **4a-c** (1eq.) was slowly added without solvent. NaI was equally added without solvent (1 eq.) and the mixture was then refluxed for 1 days. The reaction was quenched by few mL of MeOH and the solution was extracted with Et_2O. The organic phase was washed with water, dried over $MgSO_4$, filtered and concentrated to give the crude compounds **5a-c**. The product was purified by chromatography on silica gel (Eluent: toluene/ Et_2O (9:1)) to give the pure compounds **5a-c** between 32% and 88% yield as a yellow oil.

4.1.2.1 2,2-Dimethyl-4-(((4-(pyren-1-yl)butyl)oxy)methyl)-1,3-dioxolane (**5a**)

Using the aforementioned general procedure, the compound **5a** was prepared in 32% yield (480mg). Rf (Eluent : toluene / Et_2O (95/5)) : 0.47; ^{1}H NMR ($CDCl_3$, 300.131 MHz): 8.27-8.25 (d, 1H, H_{ar}, J_{HH}=8 Hz); 8.16-7.96 (m, 7H, H_{ar}); 7.86-7.84 (d, 1H, H_{ar}, J_{HH}=8 Hz); 4.27-4.21 (qt, 1H, J_{HH}= 12 Hz, J_{HH2}= 6 Hz, C*H sn-2*); 4.04-4.01 (dd, 1H, J_{HH}= 6 Hz, J_{HH}= 8 Hz, H_a C*H₂ sn-3*); 3.71-3.68 (dd, 1H, J_{HH}= 6 Hz, J_{HH}= 8 Hz, H_b C*H₂ sn-3*); 3.57-3.38 (m, 4H, C*H₂ sn-1* + C*H₂* α-solketal); 3.35 (t, 2H, J_{HH}= 7.7 Hz, CH_2 α pyrene); 1.96-1.88 (m, 2H, CH_2 fatty chain); 1.79-1.72 (m, 2H, CH_2 fatty chain); 1.40 (s, 3H, CH_3 solketal); 1.34 (s, 3H, CH_3 solketal); ^{13}C NMR ($CDCl_3$, 75.474 MHz): 136.9 (C_q); 131.60 (C_q); 131.09 (C_q); 129.92 (C_q); 128.78 (C_q); 127.67-125.94 (CH pyrene); 125.25 (C_q); 124.98-123.58 (CH pyrene); 109.52 (*C_q* solketal); 74.89 (*CH sn-2*); 72.09 (*C*H₂ *sn-1*); 71.73 (CH_2 α O); 67.04 (*C*H₂ *sn-3*); 33.44 (CH_2 α pyrene); 29.75 (CH_2 β pyrene); 28.48 (CH_2 fatty chain); 26.93 (*C*H₃ acetal); 25.57 (*C*H₃ acetal); MALDI TOF *m/z* calculated 388.499 found $M^{+\bullet}$ 388.313.

4.1.2.2 2,2-Dimethyl-4-(((11-(pyren-1-yl)undecyl)oxy)methyl)-1,3-dioxolane (**5b**)

Using the aforementioned general procedure, the compound **5b** was prepared in 88% yield (5.2g). Rf (Eluent : toluene / Et_2O (9/1)) : 0.37; ^{1}H NMR ($CDCl_3$, 399.922 MHz): 8.3 (d, 1H, H_{ar}, J_{HH}= 9.2 Hz); 8.17-7.86 **5** (m, 8H, H_{ar}); 4.28 (qt, 1H, J_{HH}= 6.4 Hz, C*H sn-2*); 4.07 (dd, 1H, J_{HH}= 6.4Hz, J_{HH}= 8.4 Hz, H_a C*H₂ sn-3*); 3.74 (dd, 1H, J_{HH}= 6.4 Hz, J_{HH}= 8.4 Hz, H_b C*H₂ sn-3*); 3.65 (t, 2H, J_{HH}= 6.8 Hz, C*H₂* α-OH); 3.53-3.39 (m, 4H, C*H₂ sn-1* + C*H₂* α-solketal); 3.34 (t, 2H, J_{HH}= 7.6 Hz, CH_2 α pyrene); 1.85 (m, 2H, CH_2 fatty chain); 1.6 (m, 2H, CH_2 fatty chain); 1.5 (m, 2H, CH_2 fatty chain); 1.45 (s, 3H, CH_3 solketal); 1.39 (s, 3H, CH_3 solketal); 1.29 (m, 14H, CH_2 fatty chain); ^{13}C NMR ($CDCl_3$, 75.474 MHz): 137.3 (C_q); 131.38 (C_q); 130.9 (C_q); 129.63 (C_q); 127.56 (C_q); 127.49-124.69 (CH pyrene); 125.03 (C_q); 124.55-123.48 (CH pyrene); 109.31 (*C_q solketal*); 74.73 (*CH sn-2*); 71.8 (*C*H₂ *sn-1*); 71.77 (CH_2 α O); 66.90 (*C*H₂ *sn-3*); 32.57 (CH_2 α pyrene); 31.91 (CH_2 β pyrene); 29.79-29.41 (CH_2 fatty chain); 26.75 (*C*H₃ acetal); 26.01 (*C*H₂ fatty chain); 25.40 (*C*H₃ acetal); MALDI TOF *m/z* calculated 486.313 found $[M+H]^+$ 487.350.

4.1.2.3 2,2-Dimethyl-4-(((16-(pyren-1-yl)hexadecyl)oxy)methyl)-1,3-dioxolane (**5c**)

Using the aforementioned general procedure, the compound **5c** was prepared in 89% yield (5g). Rf (Eluent: toluene / Et_2O (95/5)): 0.53; ^{1}H NMR ($CDCl_3$, 300.131 MHz): 8.3 (d, 1H, H_{ar}, J_{HH}=12 Hz); 8.17-7.86 (m, 8H, H_{ar}); 4.25 (qt, 1H, J_{HH}= 7 Hz, C*H sn-2*); 4.07 (dd, 1H, J_{HH}= 6.4 Hz, J_{HH}= 8.4 Hz, H_a C*H₂ sn-3*); 3.74 (dd, 1H, J_{HH}= 6.4 Hz, J_{HH}= 8.4 Hz, H_b C*H₂ sn-*

3); 3.53-3.39 (m, 4H, C*H₂ sn-1* + C*H₂* α-solketal); 3.34 (t, 2H, J_{HH}= 7.6 Hz, CH_2 α pyrene); 1.86 (m, 2H, CH_2 fatty chain); 1.6 (m, 2H, CH_2 fatty chain); 1.5 (m, 2H, CH_2 fatty chain); 1.45 (s, 3H, CH_3 solketal); 1.39 (s, 3H, CH_3 solketal); 1.26 (s, 21H, CH_2 fatty chain); ^{13}C NMR ($CDCl_3$, 75.474 MHz): 137.5 (C_q); 131.61 (C_q); 131.07 (C_q); 129.83 (C_q); 128.80(C_q); 127.65-125.85 (CH pyrene); 125.28 (C_q); 124.87-123.65 (CH pyrene); 109.47 (*C_q solketal*); 74.88 (*CH sn-2*); 72.01 (*C*H_2 *sn-1*); 71.94 (CH_2 α O); 67.06 (*C*H_2 *sn-3*); 33.75 (CH_2 α pyrene); 32.08 (CH_2 β pyrene); 29.96-29.59 (CH_2 fatty chain); 26.90 (*C*H_3 acetal); 26.18 (*C*H_2 fatty chain); 25.56 (*C*H_3 acetal); MALDI TOF *m/z* calculated 556.392 found $M^{+\bullet}$ 556.559.

4.1.3 General procedure for the acetal function deprotection (Compounds **6a-c**)

Acetic acid 80% (60 mL) and 15 mL of H_2O were added to **5a-c** (1 eq.). The mixture was stirred for 3 hours at 50°C. Acetic acid and water were distilled under vacuum to produce compounds **6a-c** between 88 and 100% yield as yellow solid. These compounds were used in the next step without further purification.

4.1.3.1 3-((4-(Pyren-1-yl)butyl)oxy)propane-1,2-diol (**6a**)

Using the aforementioned general procedure, the compound **6a** was prepared in 88% yield (0.380g). Rf TLC (Eluent: toluene / Et_2O (3/7)) : 0.2; ^1H NMR ($CDCl_3$, 399.922 MHz): 8.27.8.25 (d, 1H, H_{ar}, J_{HH}= 9.0 Hz); 8.18-7.97 (m, 7H, H_{ar}); 7.86-7.84 (d, 1H, J_{HH}= 7.7 Hz, H_{ar}); 3.88-3.83 (qt, 1H, J_{HH}= 5.6 Hz, C*H sn-2*); 3.71-3.32 (m, 8H, C*H₂ sn-3* +C*H₂ sn-1* + C*H₂* α-solketal + CH_2 α pyrene); 2.09 (s, 2H, OH); 1.94-1.87 (m, 2H, CH_2 fatty chain); 1.77-1.71 (m, 2H, CH_2 fatty chain); ^{13}C NMR ($CDCl_3$, 75.474MHz): 136.63 (C_q); 131.50 (C_q); 130.96 (C_q); 129.89 (C_q); 128.67 (C_q); 127.58 - 125.88 (CH pyrene); 125.15 (C_q); 124.94 – 123.40 (CH pyrene); 72.39 (*C*H_2 *sn-1*); 72.39 (CH_2 α O); 71.56 (CH_2 α solketal); 70.68 (*CH sn-2*); 64.14 (*C*H_2 *sn-3*); 33.27 (CH_2 α pyrene); 29.59 (CH_2 β pyrene); 28.28 (CH_2 fatty chain);

4.1.3.2 3-((11-(Pyren-1-yl)undecyl)oxy)propane-1,2-diol (**6b**)

Using the aforementioned general procedure, the compound **6b** was prepared in quantitative yield (5.5g)**.** Rf TLC (Eluent: toluene / Et_2O (1/1)): 0.15; Melting point : 56°C; ^1H NMR ($CDCl_3$, 399.922 MHz): 8.3 (d, 1H, H_{ar}, J_{HH}= 9.2 Hz); 8.17-7.97 (m, 7H, H_{ar}); 7.87 (d, 1H, J_{HH}= 7.6 Hz, H_{ar}); 3.86 (m, 1H, C*H sn-2*); 4.07 (m, 2H, C*H₂ sn-3*); 3.50-3.41 (m, 5H, C*H₂ sn-1* + C*H₂* α-solketal); 3.34 (t, 2H, J_{HH}= 8 Hz, CH_2 α pyrene); 2.32 (s, 2H, OH); 1.85 (m, 2H, CH_2 β Solketal); 1.5 (m, 2H, CH_2 β pyrene); 1.45 (m, 2H, CH_2 γ Solketal); 1.38-1.29 (m,

12H, CH_2 fatty chain); ^{13}C NMR ($CDCl_3$, 75.474 MHz): 137.18 (C_q); 131.31 (C_q); 130.80 (C_q); 129.54 (C_q); 129.33 (C_q); 128.91-125.18 (CH pyrene); 124.94 (C_q); 124.60-123.35 (CH pyrene); 72.24 (*C*H_2 *sn-1*); 71.68 (CH_2 α solketal); 70.41 (*CH sn-2*); 64.08(*C*H_2 *sn-3*); 33.47 (CH_2 α pyrene); 31.81 (CH_2 β pyrene); 29.69-29.31 (CH_2 fatty chain) ; 25.92 (*C*H_2 fatty chain); MALDI TOF *m/z* calculated 446.282 found $M^{+\bullet}$ 446.454.

4.1.3.3 3-((16-(Pyren-1-yl)hexadecyl)oxy)propane-1,2-diol (**6c**)

Using the aforementioned general procedure, the compound **6c** was prepared in 95% yield (4.4 g). Rf TLC (Eluent: toluene / Et_2O (3/7)): 0.4; Melting point : 90°C; ^1H NMR ($CDCl_3$, 300.131 MHz): 8.3 (d, 1H, H_{ar}, J_{HH}= 9.0 Hz); 8.17-7.97 (m, 7H, H_{ar}); 7.87 (d, 1H, J_{HH}= 7.6 Hz, H_{ar}); 3.87 (m, 1H, C*H sn-2*); 3.85-3.61 (m, 2H, C*H*$_2$ *sn-3*); 3.54-3.43 (m, 4H, C*H*$_2$ *sn-1* + C*H*$_2$ α-solketal); 3.33 (t, 2H, J_{HH}= 8 Hz, CH_2 α pyrene); 2.09 (s, 2H, OH); 1.87 (m, 2H, CH_2 fatty chain); 1.56 (m, 2H, CH_2 fatty chain); 1.47 (m, 2H, CH_2 fatty chain); 1.29 (m, 21H, CH_2 fatty chain); ^{13}C NMR ($CDCl_3$, 75.474 MHz): 137.40 (C_q); 131.52 (C_q); 131.01 (C_q); 129.73 (C_q); 128.66 (C_q); 127.59-125.79 (CH pyrene); 125.14 (C_q); 124.82-123.58 (CH pyrene); 72.41 (*C*H_2 *sn-1*); 71.90 (CH_2 α solketal); 70.64 (*CH sn-2*); 64.24 (*C*H_2 *sn-3*); 33.68 (CH_2 α pyrene); 32.02 (CH_2 β pyrene); 29.92-29.56 (CH_2 fatty chain); 26.13 (*C*H_2 fatty chain); MALDI TOF *m/z* calculated 516.360 found $M^{+\bullet}$ 516.476.

4.1.4 General procedure for the primary alcohol protection with *tert*-Butyldimethylsilyle chloride (compounds **7a**, **b** and **c**)

A solution of *tert*-Butyl(chloro)dimethylsilane (1.3 eq.) and imidazole (2.5 eq.) previously mixed in anhydrous CH_2Cl_2 (20 mL) were added in solution of **6a-c** (1eq.) in CH_2Cl_2 (20 mL). The mixture was stirred for 2 hours at 40°C. The mixture was poured into water (300 mL) and extracted with Et_2O. The combined ether extracts were washed with brine, dried over Na_2SO_4, filtered and concentrated to give the crude compounds **7a-c** as yellow wax between 96% and quantitative yield. These compounds were used in the next step without further purification.

4.1.4.1 1-((*tert*-Butyldimethylsilyl)oxy)-3-((4-(pyren-1-yl)butyl)oxy)propan-2-ol (**7a**)

Using the aforementioned general procedure, the compound **7a** was prepared in 96% yield (0.480g). Rf TLC (Eluent: toluene/ ethyl acetate (4/1)): 0.6; ^1H NMR ($CDCl_3$, 399.922 MHz): 8.28 - 8.26 (d, 1H, H_{ar}, J_{HH}= 9.2 Hz); 8.16-7.96 (m, 7H, H_{ar}); 7.87-7.84 (d, 1H, J_{HH}= 7.8 Hz,

H_{ar}); 3.83 - 3.78 (qt, 1H, , J_{HH}=10.9 Hz , J_{HH}=5.3 Hz, C*H sn-2*); 3.68 – 3.41 (m, 6H, C*H₂ sn-3* + C*H₂ sn-1* + C*H₂* α-solketal); 3.36 (t, 2H, J_{HH}= 7.8 Hz, CH_2 α pyrene); 1.96 - 7.88 (m, 2H, CH_2 β pyrene); 1.79 – 1.73 (m, 2H, CH_2 β solketal); 0.87 (m, 9H, CH_3 Si-*t-Bu*); 0.04 (m, 6H, CH_3 Si); ^{13}C NMR ($CDCl_3$, 75.474 MHz): 136.72 (C_q); 131.45 (C_q); 130.93 (C_q); 129.81 (C_q); 128.62 (C_q); 127.56-125.83 (CH pyrene); 125.11 (C_q); 124.85-123.41 (CH pyrene); 71.64 (*C*H_2 *sn-1*); 71.39 (CH_2 α solketal); 70.73 (*CH sn-2*); 64.13 (*C*H_2 *sn-3*); 33.28 (CH_2 α pyrene); 29.69 (CH_2 fatty chain); 28.34 (CH_2 fatty chain); 25.93 (CH_3 Si-*t-Bu*); -5.36 (CH_3 Si) ; MALDI TOF *m/z* calculated 462.259 found $M^{+\bullet}$ 462.344 and $[M+Na]^+$ 485.335, theoretical value for $[M+Na]^+$ 485.248.

4.1.4.2 1-((*tert*-Butyldimethylsilyl)oxy)-3-((11-(pyren-1-yl)undecyl)oxy)propan-2-ol (**7b**)

Using the aforementioned general procedure, the compound **7b** was prepared in 99% yield (4.5g). Rf TLC (Eluent: toluene / ethyl acetate (4/1)) : 0.57; ^{1}H NMR ($CDCl_3$, 399.922 MHz): 8.3 (d, 1H, H_{ar}, J_{HH}= 9.2 Hz); 8.17-7.97 (m, 7H, H_{ar}); 7.87 (d, 1H, J_{HH}= 7.6 Hz, H_{ar}); 3.81 (m, 1H, C*H sn-2*); 3.64 (m, 2H, C*H₂ sn-3*); 3.46-3.42 (m, 4H, C*H₂ sn-1* + C*H₂* α-solketal); 3.34 (t, 2H, J_{HH}= 8 Hz, CH_2 α pyrene); 2.36 (s, 2H, OH); 1.85 (m, 2H, CH_2 β pyrene); 1.56 (m, 2H, CH_2 β solketal); 1.54 (m, 2H, CH_2 γ solketal); 1.36 (m, 14H, CH_2 fatty chain); 0.89 (m, 9H, CH_3 Si-*t-Bu*); 0.069 (m, 6H, CH_3 Si); ^{13}C NMR ($CDCl_3$, 75.474 MHz): 136.97 (C_q); 131.25 (C_q); 130.74 (C_q); 129.48 (C_q); 128.85 (C_q); 128.38-125.46 (CH pyrene); 125.14 (C_q); 124.89-123.23 (CH pyrene); 71.41 (*C*H_2 *sn-1*); 71.31 (CH_2 α solketal); 70.52 (*CH sn-2*); 63.97(*C*H_2 *sn-3*); 33.37 (CH_2 α pyrene); 31.71 (CH_2 β pyrene); 29.66-29.34 (CH_2 fatty chain) ; 25.97 (*C*H_2 fatty chain); 25.77 (CH_3 Si-*t-Bu*); -5.55 (CH_3 Si); MALDI TOF *m/z* calculated 560.369 found $[M+Na]^+$ 583.515, Theoretical value for $[M+Na]^+$ 583.358.

4.1.4.3 1-((*tert*-Butyldimethylsilyl)oxy)-3-((16-(pyren-1-yl)hexadecyl)oxy)propan-2-ol (**7c**)

Using the aforementioned general procedure, the compound **7c** was prepared in quantitative yield (5.2g). Rf TLC (Eluent: toluene/ Et_2O (9:1)): 0.52; ^{1}H NMR ($CDCl_3$, 300.131 MHz): 8.31 (d, 1H, H_{ar}, J_{HH}= 9.2 Hz); 8.2-7.96 (m, 7H, H_{ar}); 7.88 (d, 1H, J_{HH}= 7.6 Hz, H_{ar}); 3.84 (m, 1H, C*H sn-2*); 3.67 (m, 2H, C*H₂ sn-3*); 3.52-3.44 (m, 4H, C*H₂ sn-1* + C*H₂* α-solketal); 3.34 (t, 2H, J_{HH}= 8 Hz, CH_2 α pyrene); 2.17 (s, 1H, OH); 1.87 (m, 2H, CH_2 β pyrene); 1.59 (m, 2H, CH_2 β solketal); 1.50 (m, 2H, CH_2 α solketal); 1.28 (m, 22H, CH_2 fatty chain); 0.94 (m, 9H, CH_3 Si-*t-Bu*); 0.10 (m, 6H, CH_3 Si); ^{13}C NMR ($CDCl_3$, 75.474 MHz): 137.45 (C_q); 131.55

(C_q); 131.05 (C_q); 129.77 (C_q); 128.70 (C_q); 127.63-125.82 (CH pyrene); 125.18 (C_q); 124.85-123.62 (CH pyrene); 71.76 (*C*H_2 *sn-1*); 71.52 (CH_2 α solketal); 70.76 (*CH sn-2*); 64.18 (*C*H_2 *sn-3*); 33.72 (CH_2 α pyrene); 32.06 (CH_2 β pyrene); 29.95-29.60 (CH_2 fatty chain) ; 26.23 (*C*H_2 fatty chain); 25.99 (CH_3 Si-*t-Bu*); -5.30 (CH_3 Si) ; MALDI TOF *m/z* calculated 630.447 found $[M+Na]^+$ 653.592, Theoretical value for $[M+Na]^+$ 653.436.

4.1.5 General procedure for the methylation reaction (compounds **8a**, **b** and **c**)

To a stirred solution of **7a-c** (1eq.) previously diluted in anhydrous CH_2Cl_2 (20 mL) and placed under nitrogen atmosphere, were added silver oxide (5 eq.) and molecular sieves (~ 2 g). Iodomethane (10 eq.) was added dropwise. The mixture was refluxed for 2 days and filtered on Celite. The celite pad was washed with dichloromethane. The filtrate was concentrated to produce **8a-c** as a dark yellow wax in quantitative yield. These compounds were used in the next step without further purification.

4.1.5.1 *tert*-Butyl(2-methoxy-3-((4-(pyren-1-yl)butyl)oxy)propoxy)dimethylsilane (**8a**)

Using the aforementioned general procedure, the compound **8a** was prepared in quantitative yield (470mg). Rf TLC (Eluent**:** toluene / ethyl acetate (4/1)): 0.4; ^{1}H NMR ($CDCl_3$, 399.922 MHz): 8.17 (d, 1H, H_{ar}, J_{HH}= 7.6 Hz); 8.15-7.98 (m, 7H, H_{ar}); 7.87 (d, 1H, J_{HH}= 7.6 Hz, H_{ar}); 3.72(m, 2H, C*H sn-2* + *CH*$_a$ *sn-3*); 3.61-3.42 (m, 8H, C*H*$_b$ *sn-3* + CH_3 –OMe + C*H*$_2$ *sn-1* + C*H*$_2$ α-solketal); 3.38 (t, 2H, J_{HH}= 8 Hz, CH_2 α pyrene); 1.98-1.92 (m, 2H, CH_2 β pyrene); 1.88-1.78 (m, 2H, CH_2 β solketal); 0.94 (m, 9H, CH_3 Si-*t-Bu*); 0.10 (m, 6H, CH_3 Si); ^{13}C NMR ($CDCl_3$, 75.474 MHz): 136.89 (C_q); 131.50 (C_q); 130.98 (C_q); 129.82 (C_q); 128.68 (C_q); 127.57-126.57 (CH pyrene); 125.80 (C_q); 125.14-123.65 (CH pyrene); 81.17 (*CH sn-2*); 71.49 (*C*H_2 *sn-1*); 70.38 (CH_2 α solketal); 62.56 (*C*H_2 *sn-3*); 58.19 (CH_3 –OMe); 33.35 (CH_2 α pyrene); 29.77 + 28.45 (CH_2 fatty chain); 25.98 (CH_3 Si-*t-Bu*); -5.30 (CH_3 Si); MALDI TOF *m/z* calculated 476.275 found $[M+Na]^+$ 499.366; Theoretical value for $[M+Na]^+$ 499.264.

4.1.5.2 *tert*-Butyl(2-methoxy-3-((11-(pyren-1-yl)undecyl)oxy)propoxy)dimethylsilane (**8b**)

Using the aforementioned general procedure, the compound **8b** was prepared in quantitative yield (2g). Rf TLC (Eluent: toluene / Et_2O (9/1)) : 0.21; ^{1}H NMR ($CDCl_3$, 500.133 MHz): 8.3 (d, 1H, H_{ar}, J_{HH}=9.0 Hz); 8.17-7.96 (m, 7H, H_{ar}); 7.87 (d, 1H, J_{HH}= 7.5 Hz, H_{ar}); 3.67 (m, 2H, C*H sn-2* + *CH*$_a$ *sn-3*); 3.55 (m, 1H, C*H*$_b$ *sn-3*); 3.44 (s, 3H, CH_3 –OMe); 3.43-3.36 (m, 4H, C*H*$_2$ *sn-1* + C*H*$_2$ α-solketal); 3.34 (t, 2H, J_{HH}= 8 Hz, CH_2 α pyrene); 1.85 (m, 2H, CH_2 β

pyrene); 1.48 (m, 2H, CH_2 β solketal); 1.37 (m, 2H, CH_2 γ Solketal); 1.27 (m, 10H, CH_2 fatty chain); 0.89 (m, 9H, CH_3 Si-*t-Bu*); 0.071 (m, 6H, CH_3 Si); ^{13}C NMR ($CDCl_3$, 75.474 MHz): 137.13 (C_q); 131.33 (C_q); 130.82 (C_q); 129.56 (C_q); 128.92 (C_q); 128.47-125.20 (CH pyrene); 124.97 (C_q); 124.62-123.36 (CH pyrene); 80.99 (*CH sn-2*); 71.58 (*C*H_2 *sn-1*); 70.02 (CH_2 α solketal); 62.40 (*C*H_2 *sn-3*); 57.97 (CH_3 –OMe); 33.48 (CH_2 α pyrene); 31.82 (CH_2 β pyrene); 29.74-29.41 (CH_2 fatty chain) ; 26.05 (*C*H_2 fatty chain); 25.83 (CH_3 Si-*t-Bu*); -5.50 (CH_3 Si); MALDI TOF *m/z* calculated 574.384 found $[M+Na]^+$ 597.488; Theoretical value for $[M+Na]^+$ 597.373.

4.1.5.3 *tert*-Butyl(2-methoxy-3-((16-(pyren-1-yl)hexadecyl)oxy)propoxy)dimethylsilane (**8c**)

Using the aforementioned general procedure, the compound **8c** was prepared in quantitative yield (2g). Rf TLC (Eluent**:** toluene / ethyl acetate (4/1)) : 0.33; ^1H NMR ($CDCl_3$, 300.131 MHz): 8.3 (d, 1H, H_{ar}, J_{HH}= 9.0 Hz); 8.17-7.95 (m, 7H, H_{ar}); 7.87 (d, 1H, J_{HH}= 7.5 Hz, H_{ar}); 3.71 (m, 2H, C*H sn-2* + *CH*$_a$ *sn-3*); 3.55 (m, 1H, C*H*$_b$ *sn-3*); 3.48-3.38 (m, 7H, CH_3 –OMe + C*H*$_2$ *sn-1* + C*H*$_2$ α-solketal); 3.33 (t, 2H, J_{HH}= 8 Hz, CH_2 α pyrene); 1.86 (m, 2H, CH_2 β pyrene); 1.57 (m, 2H, CH_2 β solketal); 1.50 (m, 2H, CH_2 γ Solketal); 1.27 (m, 23H, CH_2 fatty chain); 0.93 (m, 9H, CH_3 Si-*t-Bu*); 0.10 (m, 6H, CH_3 Si); ^{13}C NMR ($CDCl_3$, 75.474 MHz): 137.47 (C_q); 131.58 (C_q); 131.07 (C_q); 129.80 (C_q); 128.72 (C_q); 127.66-125.85 (CH pyrene); 125.21 (C_q); 124.88-123.65 (CH pyrene); 81.22 (*CH sn-2*); 71.85 (*C*H_2 *sn-1*); 70.27 (CH_2 α solketal); 62.61 (*C*H_2 *sn-3*); 58.24 (CH_3 –OMe); 33.75 (CH_2 α pyrene); 32.09 (CH_2 β pyrene); 29.98-29.65 (CH_2 fatty chain); 26.28 (*C*H_2 fatty chain); 26.05 (CH_3 Si-*t-Bu*); -5.23 (CH_3 Si); MALDI TOF *m/z* calculated 644.462 found $[M+Na]^+$ 667.619; Theoretical value for $[M+Na]^+$ 667.452.

4.1.6 General procedure for the deprotection of the *tert*-Butyl-dimethylsilyle protecting group (compound **9a-c**): Tetra-n-butylammonium fluoride (5 eq.) was added to a stirred solution of **8a-c** (1 eq.) diluted in dry THF (15 mL) previously placed under nitrogen atmosphere. The reaction was stirred at room temperature overnight. The solution was quenched by addition of water (10 mL) and extracted with Et_2O (3*30 mL). The organic layer was washed with brine, dried over Na_2SO_4, filtered and concentrated to give the crude compound **9a-c**. The product was purified by chromatography on silica gel (Eluent: pentane/ ethyl acetate (3/7)) to give the pure compound **9a-c** as a yellow wax or yellow solid between 51% and 93% yield.

4.1.6.1 2-Methoxy-3-((4-(pyren-1-yl)butyl)oxy)propan-1-ol **9a -** Using the aforementioned general procedure, the compound **9a** was prepared in 51% yield (185mg). Rf TLC (Eluent**:** pentane / ethyl acetate (3/7)): 0.66; Melting point = 82°C; ^{1}H NMR ($CDCl_3$, 399.922 MHz): 8.28-8.25 (m, 1H, H_{ar}); 8.17-7.15 (m, 2H, H_{ar}); 8.11-8.08 (m, 2H, H_{ar}); 8.05-7.95 (m, 3H, H_{ar}); 7.87-7.84 (m, 1H, H_{ar}); 3.76-3.71 (m, 1H, *CH_a sn-3*); 3.65-3.60 (m, 1H, C*H_b sn-3*); 3.57-3.38 (m, 9H, C*H sn-2* + C*H_2 sn-1* + C*H_2* α-solketal + CH_3 –OMe); 3.36 (m, CH_2 α pyrene); 1.96-1.87 (m, 2H, CH_2 β pyrene); 1.80-1.72 (m, 3H, CH_2 β solketal); ^{13}C NMR ($CDCl_3$, 75.474 MHz): 136.72 (C_q); 131.46 (C_q); 130.94 (C_q); 129.82 (C_q); 128.64 (C_q); 127.55-125.81 (CH pyrene); 125.11 (C_q); 124.87-123.42 (CH pyrene); 80.01 (*CH sn-2*); 71.60 (CH_2 α solketal); 70.53 (*C*H_2 *sn-1*); 62.55 (*C*H_2 *sn-3*); 57.80 (CH_3 –OMe); 33.28 + 29.64 + 28.32 (CH_2 pyrene); MALDI TOF *m/z* calculated 362.188 found $M^{+\bullet}$ 362.287.

4.1.6.2 2-Methoxy-3-((11-(pyren-1-yl)undecyl)oxy)propan-1-ol **9b -** Using the aforementioned general procedure, the compound **9b** was prepared in 93% yield (1g). Rf TLC (Eluent: toluene / ethyl acetate (7/3)): 0.23; ^{1}H NMR ($CDCl_3$, 399.922 MHz): 8.3 (d, 1H, H_{ar}, J_{HH}= 9.2 Hz); 8.17-7.98 (m, 7H, H_{ar}); 7.88 (d, 1H, J_{HH}= 7.5 Hz, H_{ar}); 3.78-3.74 (m, 1H, *CH_a sn-3*); 3.67-3.62 (m, 1H, C*H_b sn-3*); 3.57-3.41 (m, 9H, C*H sn-2* + C*H_2 sn-1* + C*H_2* α-solketal + CH_3 –OMe); 3.34 (t, 2H, J_{HH}= 8 Hz, CH_2 α pyrene); 1.85 (m, 3H, CH_2 β pyrene); 1.56 (m, 3H, CH_2 β solketal); 1.48 (m, 3H, CH_2 γ Solketal); 1.27 (m, 11H, CH_2 fatty chain); ^{13}C NMR ($CDCl_3$, 75.474 MHz): 137.26 (C_q); 131.37 (C_q); 130.86 (C_q); 129.59 (C_q); 128.52 (C_q); 127.46-125.65 (CH pyrene); 125.0 (C_q); 124.69-123.44 (CH pyrene); 79.81 (*CH sn-2*); 71.82 (*C*H_2 *sn-1*); 70.50 (CH_2 α solketal); 62.57 (*C*H_2 *sn-3*); 57.67 (CH_3 –OMe); 33.53 (CH_2 α pyrene); 31.87 (CH_2 β pyrene); 29.75-29.37 (CH_2 fatty chain); 25.99 (*C*H_2 fatty chain); MALDI TOF *m/z* calculated 460.298 found $M^{+\bullet}$ 460.474.

4.1.6.3 2-Methoxy-3-((16-(pyren-1-yl)hexadecyl)oxy)propan-1-ol **9c -** Using the aforementioned general procedure, the compound **9c** was prepared in 51% yield (840 mg). Rf TLC (Eluent**:** pentane / ethyl acetate (1/1)): 0.77; ^{1}H NMR ($CDCl_3$, 399.922 MHz): 8.3 (d, 1H, H_{ar}, J_{HH}= 9.2 Hz); 8.16-7.95 (m, 7H, H_{ar}); 7.87 (d, 1H, J_{HH}= 7.5 Hz, H_{ar}); 3.77-3.73 (m, 1H, *CH_a sn-3*); 3.66-3.62 (m, 1H, C*H_b sn-3*); 3.57-3.39 (m, 9H, C*H sn-2* + C*H_2 sn-1* + C*H_2* α-solketal + CH_3 –OMe); 3.33 (t, 2H, J_{HH}= 8 Hz, CH_2 α pyrene); 1.85 (m, 3H, CH_2 β pyrene); 1.56 (m, 3H, CH_2 β solketal); 1.48 (m, 3H, CH_2 γ Solketal); 1.27 (m, 22H, CH_2 fatty chain); ^{13}C NMR ($CDCl_3$, 75.474 MHz): 137.43 (C_q); 131.50 (C_q); 130.99 (C_q); 129.71 (C_q); 128.64 (C_q); 127.57-125.77 (CH pyrene); 125.12 (C_q); 124.79-123.58 (CH pyrene); 79.85 (*CH sn-2*); 71.97 (*C*H_2 *sn-1*); 70.67 (CH_2 α solketal); 62.75 (*C*H_2 *sn-3*); 57.80 (CH_3 –OMe); 33.66 (CH_2

α pyrene); 32.0 (CH_2 β pyrene); 29.88-29.49 (CH_2 fatty chain); 26.11 (*C*H_2 fatty chain); MALDI TOF *m/z* calculated 530.376 found $M^{+\bullet}$ 530.469.

4.1.7 General procedure for the glycosylation reaction (compounds **10a-c**): Peracetylated lactose trichloroacetimidate (1.2 eq.) solubilized in dry CH_2Cl_2 (20 mL) was added dropwise to a solution of **9a-c** (1 eq.) in CH_2Cl_2 (15 mL). The mixture was stirred with molecular sieves (~ 2 g) during one hour under nitrogen atmosphere. At 0°C, boron trifluoride diethyl etherate (0.8 eq.) was added dropwise and the mixture was stirred overnight at RT under inert atmosphere. The mixture was quenched by addition of water (20 mL). The organic layer was washed with aqueous saturated $NaHCO_3$ solution and brine. The organic layer was dried over $MgSO_4$, filtered, concentrated to give the crude compounds **10a-c**. The product was purified by chromatography on silica gel (Eluent: pentane/ ethyl acetate (3/2)) to give the pure compounds **10a-c** as white foam between 42% and 58% yield.

4.1.7.1 1-*O*-Butylpyrene-2-*O*-methyl-*rac*-glycer-3-yl-2,3,4,6-tetra-*O*-acetyl-β-D-galactopyranosyl-(1-4)-2,3,6-tri-*O*-acetyl-β-D-glucopyranoside (**10a**)

Using the aforementioned general procedure, the compound **10a** was prepared in 42% yield (410mg). Rf TLC (Eluent: pentane/ ethyl acetate (3/7)): 0.7; ^{1}H NMR ($CDCl_3$, 500.133 MHz): 8.24 (d, 1H, H_{ar}, J_{HH}=9.6 Hz); 8.14-7.85 (m, 7H, H_{ar}); 7.84 (d, 1H, J_{HH}= 7.6 Hz, H_{ar}); 5.33 (m, 1H, $H_{4'}$); 5.16-5.13 (m, 1H, H_3); 5.10-5.07 (m, 1H, $H_{2'}$); 4.94-4.84 (m, 2H, $H_{3'}$ + H_2); 4.45-4.38 (m, 3H, H_{6a} + H_1 + $H_{1'}$); 4.1-3.99 (m, 4H, $H_{6'a}$ + $H_{6'b}$ + H_{6b} + ethyl acetate); 3.88-3.79 (m, 2H, *sn-3*$_b$ + $H_{5'}$); 3.73-3.68 (m, 1H, H_4); 3.59-3.28 (m, 12H, *sn-3*$_a$ + H_5 + -OCH_3 + CH *sn-2* + CH_2 *sn-1* + CH_2 α Solketal + CH_2 α pyrene); 2.14-1.95 (m, 21H, CH_3-OAc Lactose); 1.89 (m, 2H, CH_2 β pyrene); 1.77-1.69 (m, 2H, CH_2 β solketal); 1.24 (t, 1.5H, ethyl acetate); ^{13}C NMR ($CDCl_3$, 125.803 MHz): 171.0 (CO); 170.20 (CO); 170.02 (CO); 169.93 (CO); 169.62 (CO); 169.42 (CO); 168.95 (CO); 136.64 (C_q); 131.28 (C_q); 130.76 (C_q); 129.64 (C_q); 128.46 (C_q); 127.39-125.69 (CH pyrene); 124.92 (C_q); 124.71-123.30 (CH pyrene); 100.91 ($C_{1'}$); 100.71 + 100.66 (C_1 β anomere); 79.19 + 78.83 (C_{sn-2} – two diastereoisomers); 76.13 (C_4); 72.61 (C_3); 72.39 (C_5); 71.52 ($C_{5'}$); 71.36 (C α Solketal); 70.85 (C_2); 70.50 ($C_{3'}$); 70.1 (C *sn-3*$_a$ - two diastereoisomers); 69.83 + 69.71 (C *sn-1* - two diastereoisomers); 68.95 (C*2'*); 68.54 (C *sn-3*$_b$ - two diastereoisomers); 66.48 ($C_{4'}$); 61.8 (C_6); 60.67 ($C_{6'}$); 60.38 (ethyl acetate); 58.11 + 57.76 (C –O*Me*); 33.12 + 29.46 +28.21 (CH_2 pyrene); 20.67 + 20.48 + 20.38 (C –*OAc* Lactose); 14.05 (ethyl acetate); MALDI TOF *m/z* calculated 980.368 found $[M+Na]^+$ 1003.318, theoretical value for $[M+Na]^+$ 1003.357.

4.1.7.2 1-*O*-Undecylpyrene-2-*O*-methyl-*rac*-glycer-3-yl-2,3,4,6-tetra-*O*-acetyl-β-D-galactopyranosyl-(1-4)-2,3,6-tri-*O*-acetyl-β-D-glucopyranoside (**10b**)

Using the aforementioned general procedure, the compound **10b** was prepared in 58% yield (1.0 g). Rf TLC (Eluent: pentane/ ethyl acetate (3/2)): 0.32; ^{1}H NMR ($CDCl_3$, 500.133 MHz): 8.22 (d, 1H, H_{ar}, J_{HH}= 9.0 Hz); 8.11-7.91 (m, 7H, H_{ar}); 7.81 (d, 1H, J_{HH}= 8.0 Hz, H_{ar}); 5.32 (m, 1H, $H_{4'}$); 5.18-5.14 (m, 1H, H_3);5.11-5.07 (m, 1H, $H_{2'}$); 4.96-4.93 (m, 1H, $H_{3'}$); 4.91-4.86 (m, 1H, H_2); 4.48-4.43 (m, 3H, H_{6a} + H_1 + $H_{1'}$); 4.1-4.02 (m, 3H, $H_{6'a}$ + $H_{6'b}$ + H_{6b}); 3.88-3.79 (m, 2H, *sn-3*$_b$ + $H_{5'}$);3.75 (t, 1H, H_4); 3.58-3.50 (m, 2H, *sn-3*$_a$ + H_5); 3.44-3.33 (m, 9H, -OCH_3 + CH *sn-2* + CH_2 *sn-1* + CH_2 α Solketal); 3.27 (t, 2H, , J_{HH}= 7.8 Hz, CH_2 α pyrene); 2.13-1.95 (m, 21H, CH_3-OAc Lactose); 1.82-1.76 (m, 2H, CH_2 β pyrene); 1.53-1.49 (m, 2H, CH_2 β solketal); 1.45-1.39 (m, 2H, CH_2 γ pyrene); 1.32 (m, 2H, CH_2 γ solketal); 1.23 (m, 10H, fatty chain); ^{13}C NMR ($CDCl_3$, 125.771 MHz): 170.12 (CO); 170.09 (CO); 169.92 (CO); 169.81 (CO); 169.54 (CO); 169.31 (CO); 168.87 (CO); 137.10 (C_q); 131.21(C_q); 130.70 (C_q); 129.43 (C_q); 128.35 (C_q); 127.32-125.53(CH pyrene); 124.82 (C_q); 124.55-123.30 (CH pyrene); 100.83 ($C_{1'}$); 100.69 + 100.58 (C_1 β anomere); 79.14 + 78.77 (C_{sn-2} – two diastereoisomers); 76.10 (C_4); 72.61 (C_3); 72.39 (C_5); 71.56 (C α Solketal); 71.49 ($C_{5'}$); 70.78 (C_2); 70.44 ($C_{3'}$); 70.08 (C *sn-3*$_a$ - two diastereoisomers); 69.72 + 69.62 (C *sn-1* - two diastereoisomers); 68.93 (C*2'*); 68.52 (C *sn-3*$_b$ - two diastereoisomers); 66.47 ($C_{4'}$); 61.87 (C_6); 60.66 ($C_{6'}$); 58.00 + 57.66 (C –O*Me*); 33.35 (CH_2 α pyrene); 31.70 (CH_2 β pyrene); 29.58 + 29.36 + 29.23 (CH_2 fatty chain); 25.85 (*C*H_2 fatty chain); 20.60 + 20.40 + 20.29 (C –*OAc* Lactose); MALDI TOF *m/z* calculated 1078.477 found $[M+Na]^+$ 1101.513, theoretical value for $[M+Na]^+$ 1101.467.

4.1.7.3 1-*O*-Hexadecylpyrene-2-*O*-methyl-*rac*-glycer-3-yl-2,3,4,6-tetra-*O*-acetyl-β- D-galactopyranosyl-(1-4)-2,3,6-tri-*O*-acetyl-β-D-glucopyranoside (**10c**)

Using the aforementioned general procedure, the compound **10c** was prepared in 44% yield (805mg). Rf TLC (Eluent: pentane/ ethyl acetate (7/3)): 0.14; ^{1}H NMR ($CDCl_3$, 399.922 MHz): 8.24 (d, 1H, H_{ar}, J_{HH}=9.6 Hz); 8.11-7.91 (m, 7H, H_{ar}); 7.82 (d, 1H, J_{HH}= 7.6 Hz, H_{ar}); 5.31 (m, 1H, $H_{4'}$); 5.19-5.14 (m, 1H, H_3);5.10-5.06 (m, 1H, $H_{2'}$); 4.94-4.90 (m, 1H, $H_{3'}$); 4.88-4.84 (m, 1H, H_2); 4.49-4.43 (m, 3H, H_{6a} + H_1 + $H_{1'}$); 4.1-4.01 (m, 3H, $H_{6'a}$ + $H_{6'b}$ + H_{6b}); 3.88-3.79 (m, 2H, *sn-3*$_b$ + $H_{5'}$); 3.75 (t, 1H, J_{HH}= 9.2 Hz, H_4); 3.59-3.50 (m, 2H, *sn-3*$_a$ + H_5); 3.45-3.38 (m, 9H, -OCH_3 + CH *sn-2* + CH_2 *sn-1* + CH_2 α Solketal); 3.28 (t, 2H, J_{HH}= 8.0 Hz, CH_2 α pyrene); 2.13-1.93 (m, 21H, CH_3-OAc Lactose); 1.82-1.76 (m, 2H, CH_2 β pyrene); 1.53-1.49 (m, 2H, CH_2 β solketal); 1.45-1.39 (m, 2H, CH_2 γ pyrene); 1.32 (m, 2H, CH_2 γ

solketal); 1.19 (m, 24H, fatty chain); ^{13}C NMR ($CDCl_3$, 75.474 MHz): 170.36 (CO); 170.16 (CO); 170.06 (CO); 169.78 (CO); 169.56 (CO); 169.10 (CO); 137.37 (C_q); 131.47 (C_q); 130.96 (C_q); 129.69 (C_q); 128.61 (C_q); 127.56-125.77 (CH pyrene); 125.08 (C_q); 124.79-123.55 (CH pyrene); 101.09 ($C_{1'}$); 100.95 + 100.85 (C_1 β anomere); 79.14 + 79.03 (C_{sn-2} – two diastereoisomers); 76.34 (C_4); 72.85 (C_3); 72.65 (C_5); 71.83(C α Solketal); 71.74 ($C_{5'}$); 71.03 (C_2); 70.70 ($C_{3'}$); 70.36 (C *sn-3*$_a$ - two diastereoisomers); 69.99 + 69.88 (C *sn-1* - two diastereoisomers); 69.17 (C*2'*); 68.79 (C *sn-3*$_b$ - two diastereoisomers); 66.68 ($C_{4'}$); 62.09 (C_6); 60.87($C_{6'}$); 60.38 (ethyl acetate); 58.27 + 57.93 (C –O*Me*); 33.62 (CH_2 α pyrene); 31.97 (CH_2 β pyrene); 29.85 + 29.69 + 29.51 (CH_2 fatty chain) ; 26.11 (*C*H_2 fatty chain); 21.04 + 20.84 + 20.64 + 20.53 (C –*OAc* Lactose); 14.22 (ethyl acetate); MALDI TOF *m/z* calculated 1148.556 found $[M+Na]^+$ 1171.381 and $[M+K]^+$ 1187.343, theoretical value for $[M+Na]^+$1171.545, theoretical value for $[M+K]^+$ 1187.519.

4.1.8 General procedure for final deprotection of peracetylated lactose (Compounds **OP1-3**):

Potassium carbonate (0.5 eq) was added to a stirred solution of **OP1-3** (1 eq.) diluted in anhydrous MeOH (15 mL). The mixture was stirred for 6 hours at RT. The mixture is quenched by addition of a little amount of Amberlite (IR120H) (~ 300 mg) and the solution was stirred for 30 minutes. Then, the solution was filtered on a sintered funnel and the solvent was evaporated to produce compounds **OP1-3** between 71% and 93 % yield as a white powder.

4.1.8.1 1-*O*-Butylpyrene-2-*O*-methyl-*rac*-glycer-3-yl-β-D-galactopyranosyl-(1-4)-β-D-glucopyranoside (**OP1**)

Using the aforementioned general procedure, the compound **OP1** was prepared in 73% yield (102mg). ^1H NMR (DMSO, 500.133 MHz): 8.36 (d, 1H, H_{ar}, J_{HH}= 9.2 Hz); 8.29-8.21 (m, 4H, H_{ar}); 8.14-8.11 (m, 2H, H_{ar}); 8.07-8.05 (m, 1H, H_{ar}); 7.96-7.95 (m, 1H, H_{ar}); 4.20-4.19 (m, 2H, H_1 + $H_{1'}$); 3.79-3.72 (m, 2H, H_{6a} + CH_2 *sn-3*$_a$); 3.61-3.16 (m, 25H, H_3 + H_4 + H_5 + H_{6b} + $H_{2'}$ + $H_{3'}$ + $H_{4'}$ + $H_{5'}$ + $H_{6'a}$ + $H_{6'b}$ + CH_3 – OMe (two diastereoisomers) + CH_2 α Solketal + CH_2 α pyrene + CH sn-2 + CH_2 *sn-3*$_b$ + CH_2 *sn-1*); 3.01 (t, 1H, J_{HH} = 8 Hz, H_2); 1.84-1.81 (m, 2H, CH_2 β pyrene) ; 1.67-1.65 (m, 2H, CH_2 β solketal); ^{13}C NMR (DMSO, 125.771 MHz): 136.97 (C_q); 130.88 (C_q); 130.41 (C_q); 129.20 (C_q); 128.05 (C_q); 127.46-124.76 (CH pyrene); 124.21 (C_q); 124.15 (Cq); 123.50 (CH pyrene); 103.85 ($C_{1'}$); 102.95 + 102.89 (C_1 β anomere

– two diastereoisomers); 80.73 (C_4); 78.73 + 78.67 (*C sn-2* – two diastereoisomers); 75.50 + 74.97 + 74.84 + 73.22 + 73.10 ($C_3 + C_5 + C_{2'} + C_{3'} + C_2$); 70.52 ($C_{5'}$); 70.37 (C α Solketal); 69.83 (C *sn-1* - two diastereoisomers); 68.63 + 68.41 (C *sn-3* - two diastereoisomers); 68.12 ($C_{4'}$); 60.47 (C_6); 60.38 ($C_{6'}$); 57.11 + 57.02 (C –O*Me*); 32.34 + 29.09 + 28.18 (CH_2 fatty chain); MALDI TOF *m/z* calculated 686.294 found $[M+Na]^+$ 709.346, theoretical value for $[M+Na]^+$ 709.283, found $[M+K]^+$ 725.308, theoretical value for $[M+K]^+$ 725.257.

4.1.8.2 1-*O*-Undecylpyrene-2-*O*-methyl-*rac*-glycer-3-yl-β-D-galactopyranosyl-(1-4)-β-D-glucopyranoside (**OP2**)

Using the aforementioned general procedure, the compound **OP2** was prepared in 93% yield (530mg). ^{1}H NMR (DMSO, 500.253 MHz): 8.33 (d, 1H, H_{ar}, J_{HH}=9.5 Hz); 8.26-8.02 (m, 7H, H_{ar}); 7.93 (d, 1H, J_{HH}= 8.0 Hz, H_{ar}); 5.08 (m, 2H, OH); 4.66-4.52 (m, 5H, OH); 4.20-4.17 (m, 2H, $H_1 + H_{1'}$); 3.77-3.72 (m, 2H, H_{6a} + CH_2 *sn-3*$_a$); 3.60-3.26 (m, 25H, $H_3 + H_4 + H_5 + H_{6b} + H_{2'} + H_{3'} + H_{4'} + H_{5'} + H_{6'a} + H_{6'b}$ + CH_3 – OMe (two diastereoisomers) + CH_2 α Solketal + CH_2 α pyrene + CH sn-2 + CH_2 *sn-3*$_b$ + CH_2 *sn-1*); 3.0 (t, 1H, J_{HH} = 7.8 Hz, H_2); 1.79-1.73 (m, 2H, CH_2 β pyrene); 1.46-1.38 (m, 4H, CH_2 β solketal + CH_2 γ pyrene); 1.34-1.28 (m, 2H, CH2 γ Solketal); 0.83 (m, 10H, CH_2 fatty chain); ^{13}C NMR (DMSO, 125.804 MHz): 137.07 (C_q); 130.86 (C_q); 130.38 (C_q); 129.13 (C_q); 127.98 (C_q); 127.42-124.19 (CH pyrene); 124.18 (C_q); 124.14 (C_q); 123.44 (CH pyrene); 103.83 ($C_{1'}$); 102.92 + 102.85 (C_1 β anomere – two diastereoisomers); 80.73 (C_4); 78.73 + 78.71 (*C sn-2* – two diastereoisomers); 75.48 + 74.95 + 74.79 + 73.08 ($C_3 + C_5 + C_{2'} + C_{3'}$); 73.2 ($C_2$); 70.54 (C α Solketal); 70.50 ($C_{5'}$); 69.81 (C *sn-1* - two diastereoisomers); 68.66 + 68.41 (C *sn-3* - two diastereoisomers); 68.09 ($C_{4'}$); 60.47 (C_6); 60.35 ($C_{6'}$); 57.10 + 57.01 (C –O*Me*); 32.60 (CH_2 α pyrene); 31.49 (CH_2 β pyrene); 29.13 + 28.96 + 28.92 + 28.90 + 28.80 (CH_2 fatty chain); 25.58 (*C*H_2 fatty chain); MALDI TOF *m/z* calculated 784.403 found $[M+Na]^+$ 807.443, theoretical value for $[M+Na]^+$ 807.393.

4.1.8.3 1-*O*-Hexadecylpyrene-2-*O*-methyl-*rac*-glycer-3-yl-β-D-galactopyranosyl-(1-4)-β-D-glucopyranoside (**OP3**)

Using the aforementioned general procedure, the compound **OP3** was prepared in 71% yield (420mg). ^{1}H NMR (DMSO, 500.133 MHz): 8.33 (d, 1H, H_{ar}, J_{HH}=9.5 Hz); 8.26-8.04 (m, 7H, H_{ar}); 7.93 (d, 1H, J_{HH}= 8.0 Hz, H_{ar}); 5.1-5.07 (m, 2H, OH); 4.77-4.49 (m, 5H, OH); 4.19-4.18 (m, 2H, $H_1 + H_{1'}$); 3.76-3.73 (m, 2H, H_{6a} + CH_2 *sn-3*$_a$); 3.60-3.29 (m, 25H, $H_3 + H_4 + H_5 + H_{6b} + H_{2'} + H_{3'} + H_{4'} + H_{5'} + H_{6'a} + H_{6'b}$ + CH_3 – OMe (two diastereoisomers) + CH_2 α

Solketal + CH_2 α pyrene + CH sn-2 + CH_2 *sn-3*$_b$ + CH_2 *sn-1*); 2.99 (t, 1H, J_{HH} = 7.8 Hz, H_2); 1.78-1.75 (m, 2H, CH_2 β pyrene) ; 1.44-1.41 (m, 4H, CH_2 β solketal + CH_2 γ pyrene); 1.33-1.32 (m, 2H, CH_2 γ Solketal); 1.19 (m, 20H, CH_2 fatty chain); ^{13}C NMR (DMSO, 125.771 MHz): 137.07 (C_q); 130.88 (C_q); 130.39 (C_q); 129.15 (C_q); 127.99 (C_q); 127.43-123.44 (CH pyrene); 124.15 (C_q); 123.44 (CH pyrene); 103.84 ($C_{1'}$); 102.93 + 102.86 (C_1 β anomere – two diastereoisomers); 80.73 (C_4); 78.72 + 78.67 (*C sn-2* – two diastereoisomers); 75.49 + 74.96 + 74.82 + 73.09 (C_3 + C_5 + $C_{2'}$ + $C_{3'}$); 73.21 (C_2); 70.56 (C α Solketal); 70.51 ($C_{5'}$); 69.84 (C *sn-1* - two diastereoisomers); 68.66 + 68.42 (C *sn-3* - two diastereoisomers); 68.11 ($C_{4'}$); 60.48 (C_6); 60.36 ($C_{6'}$); 57.11 + 57.02 (C –O*Me*); 32.61 (CH_2 α pyrene); 31.49 (CH_2 β pyrene); 29.16 + 28.97 + 28.86 + 28.83 (CH_2 fatty chain); 25.60 (*C*H_2 fatty chain); MALDI TOF *m/z* calculated 854.482 found $[M+Na]^+$ 877.475, theoretical value for $[M+Na]^+$ 877.471, found $[M+K]^+$ 893.437, theoretical value for $[M+K]^+$ 893.445.

4.2 Fluorescence and liposomal formulations

Fluorescence was recorded on *Agilent* Cary *Eclipse* Fluorescence Spectrophotometer. Samples were excited at 331 nm in quartz cells. Stock solutions of **OP** compounds were prepared in methanol at 50 µM. EggPC, DOPC and cholesterol were purchased from Sigma-Aldrich. EggPC (ref 840051) is a mixture of PC whose molecular weight is 770 g/mol. It contains mainly $C_{16:0}$ (32.7%), $C_{18:1}$ (32%), $C_{18:2}$ (17.1 %), $C_{18:0}$ (12.3%), $C_{20:4}$ (2.7%), $C_{16:1}$ (1.1%). Stock solutions of EggPC, DOPC and cholesterol were prepared in chloroforme at 1 mmol/L. For mixtures of EggPC or DOPC with cholesterol, stock solutions of the mixture were prepared containing 30% of cholesterol and 70% of either EggPC or DOPC (mol/mol). An aliquot of these lipids solutions was introduced in a glass tube and solvent was evaporated under vacuum. After solvent removal, pure water was added and let at 4°C for 5 nights. The samples were then warmed, vortexed, sonicated for 10 minutes. After 3 hours they were vortexed again and fluorescence was measured. The final concentration of lipids is either 8 µM or 40 µM.
For pre-insertion experiments, stock solutions of one of the **OP** compounds (10 µL) were added before evaporation of the solvent. For post-insertion they were added after sonication. The final concentration of **OP 1**, **2** or **3** was always 0.2 µM (lipid/OP ratios = 40 or 200).

4.3 Cell culture

MDA-MB-435s and HEK cell line that sur-expressed SK3 channels were cultured as already described [14]. All cell lines were obtained from the American Type Culture Collection (ATCC, LGC Promochem, Molsheim, France).

4.4 Cell migration

Cell migration assays were analyzed in 24-well plates receiving 8 µm pore size cell culture inserts (Becton Dickinson, France), as described [14]. Compounds OP1-3 were solubilized in DMSO to prepare stock solution at 10 mM.

4.5 Cell viability.

Cell viability assays were determined using MTT assay as already described [14]. Cells were seeded on 24-well plates and grown for 24 h. Compounds **OP1-3** were then added for 48 h at 1 µM.

4.6 Electrophysiology

Whole-cell SK3 currents were captured using 1322-A Digidata converter (Axon Instruments, USA) and pClamp 8.1 software (Axon Instruments, USA) as described [14]. Compounds OP1-3 were solubilized in DMSO to prepare stock solution at 10 mM.

4.7 Proteinase K digestion and Western blot

Proteinase K digestion was performed as described previously [25]. Briefly, cells were incubated with or without 200 µg/ml proteinase K (Sigma-Aldrich, France) at 37°C for 30 min and the digestion was quenched by adding ice-cold PBS containing 6 mM phenylmethylsulfonyl fluoride and 25 mM EDTA. SK3 bands were revealed using Western blot experiments as already described [25].

4.8 Cell culture and imaging

100.000 MDA-MB-231 cells were seeded in 35 mm dishes in 1 mL serum-supplemented DMEM. Cells were treated with **OP2** 24h after seeding. The stock solution of **OP2** was prepared in DMSO/EtOH (60/40) at 1 mM. This solution was diluted either 1000 or 100 times for the experiments at 1 to 10 µM. For observation immediately after treatment, the serum-containing culture medium was replaced with serum-free DMEM before adding **OP2** at the required concentration; for observation 24h after treatment, **OP2** was added to the serum-supplemented DMEM.

Cells were imaged on a wide-field Leica microscope endowed with an EM-CCD (Andor DU8285) through an oil immersion 20x microscope objective (HC PL APO 20/0.70 IMM). **OP2** fluorescence was excited at 340 nm and emission was imaged from 468 to 552 nm (the emission range of pyrene excimer).

Acknowledgements

We are grateful to Ana M. Bouchet for constructive scientific discussions and critical assistance for **OP2** cellular internalization experiments and Isabelle Domingo for technical assistance. This study was funded by Institut National du Cancer (INCA N°2018-151), the University of Brest, the University of Tours, the Région Bretagne and Région Centre-Val de Loire, INSERM, CNRS, Canceropôle Grand Ouest, La Ligue Nationale Contre le Cancer and the CANCEN Association. AB is grateful for a PhD fellowship from "La Ligue contre le Cancer" and "région Bretagne" and for a mobility grant from the university of Brest. We thank the platforms (NMR and mass spectrometry) from the University of Brest.

1 E. Bates. Ion Channels in Development and Cancer. Annu. Rev. Cell Dev. Biol. 31 (2015) 231–47.

2 N. Comes, A. Serrano-Albarrás, J. Capera, C. Serrano-Novillo, E. Condom, S.R. Cajal, J.C. Ferreres, A. Felipe. Involvement of potassium channels in the progression of cancer to a more malignant phenotype. Biochim. Biophys. Acta 1848 (2015) 2477-2492.

3 N. Déliot, B. Constantin. Plasma membrane calcium channels in cancer: Alterations and consequences for cell proliferation and migration. Biochim. Biophys. Acta 1848 (2015) 2512-2522.

4 K. Morishita, K. Watanabe, H. Ichijo. Cell volume regulation in cancer cell migration driven by osmotic water flow. Cancer Science 110 (2019) 2337-2347.

5 S. Martial, Am. J. Physiol. Cell Physiol 310 (2016) C710-C727.

6 R. Peruzzo, I. Szabo. Contribution of Mitochondrial Ion Channels to Chemo-Resistance in Cancer Cells. Cancers 11 (2019) 761.

7 P. Kischel, A. Girault, L. Rodat-Despoix, M. Chamlali, S. Radoslavova, H. Abou Daya, T. Lefebvre, A. Foulon, P. Rybarczyk, F. Hague, I. Dhennin-Duthille, M. Gautier, H. Ouadid-Ahidouch. Ion Channels: New Actors Playing in Chemotherapeutic Resistance. Cancers 11 (2019) 376.

8 M. Guéguinou, A. Chantôme, G. Fromont, P. Bougnoux, C. Vandier, M. Potier-Cartereau. KCa and Ca2+ channels: The complex thought. Biochim. Biophys. Acta 1843 (2014) 2322-2333.

9 E. Lastraioli, J. Iorio, A. Arcangeli. Ion channel expression as promising cancer biomarker. Biochem. Biophys. Acta, 2015, 1848, 2685-2702.

10 H. Wulff, P. Christophersen, P. Colussi, K.G. Chandy, V. Yarov-Yarovoy. Antibodies and venom peptides: new modalities for ion channels. Nature Rev. Drug Discovery 18 (2019) 339-357.

11 A. Girault, J.P. Haelters, M. Potier-Cartereau, A. Chantome, P.A. Jaffrès, P. Bougnoux, V. Joulin, C. Vandier. Targeting SKCa Channels in Cancer: Potential New Therapeutic Approaches. Curr. Med. Chem. 19 (2012) 697-713.

12 A. Chantome, A. Girault, M. Potier, C. Collin, P. Vaudin, J.C. Pages, C. Vandier, V. Joulin. KCa2.3 channel-dependent hyperpolarization increases melanoma cell motility Exp Cell Res 315 (2009) 3620–3630.

13 P.A. Jaffrès, C. Gajate, A.M. Bouchet, H. Couthon-Gourvès, A. Chantôme, M. Potier-Cartereau, P. Besson, P. Bougnoux, F. Mollinedo, C. Vandier. Alkyl ether lipids, ion

channels and lipid raft reorganization in cancer therapy Pharm. Ther. 165 (2016) 114-131.

14 A. Girault, J.P. Haelters, M. Potier, A. Chantôme, M. Pineau, S. Marionneau-Lambot, T. Oullier, G. Simon, H. Couthon-Gourvès, P.A. Jaffrès, V. Joulin, B. Corbel, P. Bougnoux, C. Vandier. New Alkyl-Lipid Blockers of SK3 Channels Reduce Cancer Cell Migration and Occurrence of Metastasis. Current Cancer Drug Target 11 (2011) 1111-1125.

15 A. Chantôme, M. Potier-Cartereau, L. Clarysse, G. Fromont, S. Marionneau-Lambot, M. Guéguinou, J.C. Pagès, C. Collin, T. Oullier, A. Girault, F. Arbion, J.P. Haelters, P.A. Jaffrès, M. Pinault, P. Besson, V. Joulin, P. Bougnoux, C. Vandier. Pivotal Role of the Lipid Raft SK3-Orai1 Complex in Human Cancer Cell Migration and Bone Metastases. Cancer Research 73 (2013) 4852-61.

16 C.M. Sevrain, J.P. Haelters, A. Chantôme, H. Couthon-Gourvès, A. Girault, C. Vandier, P.A. Jaffrès. Glyco-Phospho-Glycero Ether Lipids (GPGEL): synthesis and evaluation as small conductance Ca2+-activated K+ channel (SK3) inhibitors. MedChemComm. 3 (2012) 1471-1478.

17 C.M. Sevrain, J.P. Haelters, A. Chantôme, H. Couthon-Gourvès, M. Gueguinou, M. Potier-Cartereau, C. Vandier, P.A. Jaffrès. DiGalactosyl-Glycero-Ether Lipid: synthetic approaches and evaluation as SK3 channel inhibitor. Org. Biomol. Chem. 11 (2013) 4479-4487.

18 W. Berthe, C.M. Sevrain, A. Chantôme, A.M. Bouchet, M. Gueguinou, Y. Fourbon,M. Potier-Cartereau, J.P. Haelters, H.Couthon-Gourvès, C. Vandier, P.A. Jaffrès. New Disaccharide-Based Ether Lipids as SK3 Ion Channel Inhibitors. ChemMedChem 11 (2016) 1531-1539.

19 S. Kouba, J. Braire, R. Félix, A. Chantôme, P.A. Jaffrès, J. Lebreton, D. Dubreuil, M. Pipelier, X. Zhang, M. Trebak, C. Vandier, M. Mathé-Allainmat, M. Potier-Cartereau. Lipidic alkaloids as SK3 channel modulators. Synthesis and biological evaluation of 2-substituted tetrahydropyridine derivatives with potential anti-metastatic activity. Eur. J. Med. Chem. 186 (2020) 111854.

20 M.J. Lenaeus, M. Vamvouka, P.J. Focia, A. Gross. Structural basis of TEA blockade in a model potassium channel. Nature Struct. Mol. Biol. 12 (2005) 454-459.

21 C. Hanselmann, S. Grissmer. Characterization of Apamin-Sensitive Ca(2+)-activated Potassium Channels in Human Leukaemic T Lymphocytes. J. Physiol.496 (1996) 627-637.

22 F. Herrera, C.M. Sevrain, P.A. Jaffrès, H. Couthon-Gourvès, A. Grélard, E.J. Dufourc, A. Chantôme, M. Potier-Cartereau, C. Vandier, A. Bouchet. Singular Interaction between an Antimetastatic Agent and the Lipid Bilayer: The Ohmline Case. ACS Omega 2 (2017) 6361-637.

23 M. Guéguinou, T. Harnois, D. Crottes, N. Deliot, A. Gambade, A. Chantôme, J.P. Haelters, P.A. Jaffrès, M.L. Jourdan, G. Weber, P. Bougnoux, O. Mignen, N. Bourmeyster, B. Constantin, T. Lecomte, C. Vandier, M. Potier-Cartereau. SK3/TRPC1/Orai1 complex regulates SOCE-dependent colon cancer cell migration: a novel opportunity to modulate anti-EGFR mAb action by the alkyl-lipid Ohmline. Oncotarget 7 (2016) 36168-36184.

24 T. Schubert, W. Römer. How synthetic membrane systems contribute to the understanding of lipid-driven endocytosis. Biochem. Biophys. Acta 1853 (2015) 2992-3005.

25 M. Potier, A. Chantome, V. Joulin, A. Girault, S. Roger, P. Besson, M.L. Jourdan, J.Y. Le Guennec, P. Bougnoux, C. Vandier. The SK3/KCa2.3 potassium channel is a new cellular target for edelfosine. Br. J. Pharmacol. 162 (2011) 464-79.

26 E. Quesada, J. Delgado, C. Gajate, F. Mollinedo, A.U. Acuna, F. Amat-Guerri. Fluorescent Phenylpolyene Analogues of the Ether Phospholipid Edelfosine for the Selective Labeling of Cancer Cells. J. Med. Chem. 47 (2004) 5333-5335.

27 F. Mollinedo, M. Fernandez, V. Hornillos, J. Delgado, F. Amat-Guerri, A.U. Acuna, T. Nieto-Miguel, J.A. Villa-Pulgarin, C. Gonzalez-Garcia, V. Cena, C. Gajate. Involvement of lipid rafts in the localization and dysfunction effect of the antitumor ether phospholipid edelfosine in mitochondria. Cell Death Dis. 2 (2011) e158.

28 P. Somerharju. Pyrene-labeled lipids as tools in membrane biophysics and cell biologyChem. Phys. Lipids 116 (2002) 57-74.

29 J. Duhamel. New Insights in the Study of Pyrene Excimer Fluorescence to Characterize Macromolecules and their Supramolecular Assemblies in Solution. Langmuir 28 (2012) 6527-6538.

30 D. Afonso, T. Le Gall, H. Couthon-Gourvès, A. Grélard, S. Prakash, M. Berchel, N. Kervarec, E.J. Dufourc, T. Montier, P.A. Jaffrès. Triggering bilayer to inverted-hexagonal nanostructure formation by thiol–ene click chemistry on cationic lipids: consequences on gene transfection. Soft Matter 12 (2016) 4516-4520.

31 M. Sakomura, T. Nakashima, K. Ueda, M. Fujihira. Unique fluorescence spectra of a disubstituted pyrene surfactant in Langmuir–Blodgett films. *Coll. Surf. A: Physicochem. Eng. Aspects* 284-285 (2006) 528-531.

32 Z. Wang, Y. Yu, D. Zhang, D. Zhu. Thymine and adenine derivatives with pyrene, tetrathiafulvalene and nitronyl nitroxide units: Synthesis and formation of ensembles sensing thymine and adenine molecules. Chinese Sci. Bull. 51 (2006) 1947-1954.

33 K. Hayashi, Y. Mitsuyoshi, T. Kamei, T. Shimanouchi, K. Suga, Y. Okamoto, H. Nakamura, H. Umakoshi. Design of Pyrene–Fatty Acid Conjugates for Real-Time Monitoring of Drug Delivery and Controllability of Drug Release. ACS Omega 3 (2018) 3572-3580.

34 K. Furuta, K. Tomokiyo, M.T. Kuo, T. Ishikawa, M. Suzuki. Molecular Design of Glutathione-derived Biochemical Probes targeting the GS.X Pump. Tetrahedron 55 (1999) 7529-7540.

35 C. Bombelli, F. Bordi, S. Borocci, M. Diociaiuti, R. Lettieri, F. Limongelli, G. Mancini, S. Sennato. New pyrenyl fluorescent amphiphiles: synthesis and aggregation properties. Soft Matter 7 (2011) 8525-8534.

36 K. Yahata, N. Ye, K. Iso, Y. Ai, J. Lee, Y. Kishi. Stereocontrolled Synthesis of Left Halves of Halichondrins. J. Org. Chem. 82 (2017) 8808-8830.

37 D. Qin, H.S. Byun, R. Bittman. Synthesis of Plasmalogen via 2,3-Bis-O-(4¢-methoxybenzyl)-sn-glycerol. J. Am. Chem. Soc. 121 (1999) 662-668.

38 K. Lu, M. Huang, Z. Xiang, Y. Liu, J. Chen, Z. Yang. Development of a Concise and Diversity-Oriented Approach for the Synthesis of Plecomacrolides via the Diene–Ene RCM. Org. Lett. 8 (2006) 1193-1196.

39 C.H. Andersson, M. Lahmann, S. Oscarson, H. Grennberg. Reversible non-covalent derivatisation of carbon nanotubes with glycosides. Soft Matter 5 (2009) 2713-2716.

40 W. A. Bubb. NMR Spectroscopy in the Study of Carbohydrates: Characterizing the Structural Complexity Concept in Magnetic Resonance Part A 19A (2003) 1-19.

41 H. J. Pownall, L. C. Smith. Pyrene-labeled lipids: versatile probes of membrane dynamics in vitro and in living cells. Chem. Phys. Lipids 50 (1989) 191-211.

42 G. Jones, V. I. Vullev. Contribution of a Pyrene Fluorescence Probe to the Aggregation Propensity of Polypeptides. Org. Lett. 3 (2001) 2457-2460.

43 G. K. Bains, S. H. Kim, E. J. Sorin, V. Narayanaswami. The Extent of Pyrene Excimer Fluorescence Emission Is a Reflector of Distance and Flexibility: Analysis of the

Segment Linking the LDL Receptor-Binding and Tetramerization Domains of Apolipoprotein E3. Biochemistry 51 (2012) 6207-6219.

44 M.Y. Yang, A.K.S. Camara, M. Aldakkak, W.M. Kwok, D. F. Stowe. Identity and function of a cardiac mitochondrial small conductance Ca2+-activated K+ channel splice variant. Biochim. Biophys. Acta, Bioenerg. 1858 (2017) 442-458.

45 J. M. De la Fuente, S. Penadés. Synthesis of Lex-neoglycoconjugate to study carbohydrate–carbohydrate associations and its intramolecular interaction. Tetrahedron Asymmetry 13 (2002) 1879-1888.

Graphical abstract

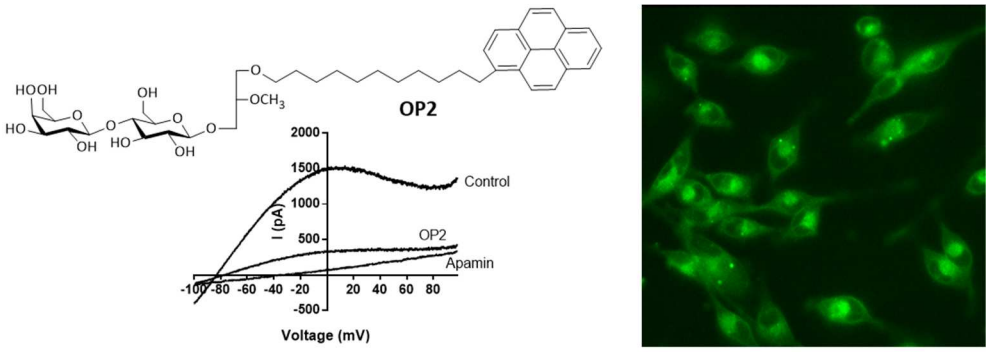

Ohmline-pyrene 2 (OP2) is the first fluorescent amphiphilic compound able to modulate SK3 channels. The kinetic of cell internalization indicates a rapid incorporation in the plasma membrane followed, after 2h, by cell internalization.